AD

TECHNICAL REPORT
71-15-FL

MICROWAVE APPLICATIONS TO FREEZE DEHYDRATION GASEOUS BREAKDOWN VS. ELECTRIC FIELD STRENGTH.

by

J. W. Gould

E. M. Kenyon

November 1970

UNITED STATES ARMY
NATICK LABORATORIES
Natick, Massachusetts 01760

FOOD LABORATORY

FL 119

AD_____

TECHNICAL REPORT

71-15-FL

MICROWAVE APPLICATIONS TO FREEZE DEHYDRATION - GASEOUS BREAKDOWN VS ELECTRIC FIELD STRENGTH

by

James W. Gould

and

Ernest M. Kenyon

Project reference:
1J662708D553

November 1970

Series: FL 119

Food Laboratory
U.S. Army Natick Laboratories
Natick, Massachusetts 01760

FOREWORD

The literature indicates that the use of microwave energy can reduce freeze-drying cycles to 1/2 - 1/10th of the time required for conventional (conductive, radiant) freeze-drying. Two of the major drawbacks to design and application of microwave energy to freeze-drying are determination of the electric field available for dielectric heating and corona breakdown (gas plasma formation). Corona breakdown can cause undesirable effects in food products during freeze-dehydration, such as deterioration of flavor components, degrading of structure and, in the extreme, burning of the food.

The author briefly reviews the theory of microwave gas breakdown and compares theoretical and literature breakdown curves for air and noble gases to show the effects of pressure, temperature, frequency, gas composition, size and shape of cavity, and electric field strength. The author then derives an equation which shows the effect of a dielectric load in the cavity on gas breakdown, and shows how this relates to heating of the dielectric load and to electric field strength.

Experimental breakdown curves for air, water and carbon dioxide are given and related to theory at 2450 MHz, the most commonly used frequency for food materials. (The literature has very sparse data on air breakdown at 2450 MHz and almost none on water or carbon dioxide breakdown at any frequency).

Pressures studied were in the range of 0.1 to 20 Torr, which covers the region of interest in practical freeze-drying. Temperatures were essentially ambient (24°C). A single cavity approximately two wavelengths on each side was used for three gases. Amperex DX206 magnetron was used with a calibrated H-tuner and dummy load to attentuate the power. A Pyrex vacuum flask inside the cavity contained the corona, and gas bleed in and hence pressure was controlled by needle valves in series. A bi-driectional coupler sampled forward and reflected power for scope display and calculation of absorbed power.

The agreement between theory and experiment is good, both for air breakdown and the effect of a dielectric load.

The results obtained show for an arbitrary microwave freeze-dryer with an arbitrary operating pressure and food load, just how much power can be applied and absorbed by the food without corona breakdown. This plus a knowledge of maximum mass transfer rates of water vapor across the dried food layer is expected to enable theoretical optimization and prediction of microwave freeze-drying rates.

Much of this work will be reported at the Fifth Annual Meeting of the International Microwave Power Institute, at The Hague, Netherlands, on October 7 - 9, 1970.

TABLE OF CONTENTS

LIST OF TABLES

LIST OF FIGURES

ABSTRACT

Food Freeze-drying cycles of 1/2 to 1/10 of the time required by conventional methods (radiant, conductive) appear feasible using microwave power. A major problem is corona breakdown, which occurs most readily under the pressure conditions of freeze-drying and causes deleterious effects on the food.

The effects of pressure, temperature, frequency, gas composition, size and shape of cavity, electric field strength, and dielectric load are explained and interrelated in the region of interest of freeze-drying, using breakdown curves from the literature and derived by the authors. Experimental breakdown curves for air, water vapor, and carbon dioxide at 2450 MHz are presented and compared with theory.

INTRODUCTION

With the Army's emphasis on freeze dried rations and the large number of units involved, any reduction in unit cost can give significant savings. This study was undertaken as a preliminary step to applying one potential method of reducing cost - that of combining microwaves and freeze drying. The usefulness of microwaves in freeze drying has been suggested and reported by numerous people 1,2,3,4. During the middle and end of the freeze dry cycle, microwaves by-pass the problem of heat conduction across the dried food layer by giving essentially volumetric heating of the receding ice layer. Thus the limiting step in the process becomes mass transfer rather than heat transfer, and depending upon the diffusivity of the food, the cycle time can be reduced by a factor of two to ten.

The basic drawbacks of the process have also been reported. Aside from equipment and electricity cost, they are:

1. Uneven electric fields - the electric field is not uniform for any general cavity. The use of mode stirrers, crossed modes, multiple inputs, and continuous processing can reduce this problem and promote even heating of the frozen food.
2. Meltback - if microwave energy is put into the food faster than the sublimation - mass transfer process can remove it, the pressure at the ice interface will rise above the triple point and the ice can melt. Aside from interrupting the freeze dry process, the microwaves will couple selectively into the water rather than the ice, causing

intense local heating, accelerated melting, and a "runaway" condition. Thus the dielectric heating rate must be matched to the maximum allowable mass flow rate to optimize the process.

3. Corona breakdown - at reduced pressures, the ionization of gas molecules by electrons accelerated in the electric field can produce a plasma formation. This gas plasma, also called a corona or glowball, will consume power meant for food heating, affect the flavor, and can even scorch the food surface if sufficiently intense. The breakdown field strength is a second upper limit to power absorption by the food (power absorption is proportional to the electric field squared).

Both 2. and 3. are related to pressure, temperature, electric field intensity, and the food loads. While pressure, temperature, and weight measurements present no real problem, the electric field is a difficult quantity to measure directly. The applicable theory in the literature does not relate well to multimode cavities and high power absorption, and requires rather sophisticated measurements of VSWR and sweep frequency half power points, methods not very applicable for industrial monitoring because of cost and untrained personnel.

This paper will instead relate food loading and electric field to power absorption, which can be measured with a forward-reverse power meter or bi-directional coupler. From this, a means of separating food power absorption from skin loss of the cavity and dielectric loss to racks, supports, etc. in the cavity will be shown. Finally, the electric breakdown fields will be compared with theory and experiment for empty cavities and loaded cavities, for varying frequencies, dielectric constants, pressures, cavities, and gases.

Thus we shall have all the data needed for process optimization except the maximum mass flow rate. The integration of this paper with the mass transfer literature is left for later work.

BASIC THEORY OF GAS BREAKDOWN

A corona discharge, or gas plasma, is a gaseous mixture of neutral gas molecules, ions, and electrons. Its most obvious characteristic is a visible glow within the microwave cavity of a color characteristic of the gas being used. Air gives a yellow-red discharge, water a reddish glow, and carbon dioxide gives a blue color. Figure 1a shows a relatively dense plasma corresponding to a high power level. As the power is decreased at constant pressure, the plasma weakens as in 1b and finally reveals the "hot spots" of maximum electric field as in Figure 1c before extinguishing.

The basic concept of plasma formation or gas breakdown is simple: free electrons are accelerated by the oscillating electric field according to the equation.

$$1. \qquad a = \frac{Eoe}{m} \sin \omega t$$

a=accel. cm/sec^2
Eo=max. electric field volts/cm.
e=electron charge coulombs
m=electron rest mass grams
ω=field frequency radians/sec

These moving electrons can have elastic or inelastic collisions with the gas molecules. In elastic collisions the electrons bounce off the atom and gain kinetic energy, but no change occurs in the internal state of the atom. After numerous elastic collisions, the electron may gain enough energy for an inelastic exciting collision. An exciting collision increases the internal energy of the atom at the expense of the electron's kinetic energy, and the electron bounces off at a slower speed. The energy is reemitted as a quantum

$h\nu$ when the excited atom relaxes to its ground state.

If the electron's kinetic energy equals the ionization potential of the gas, an inelastic ionizing collision may occur which releases two electrons, the original one plus one stripped from the neutral molecule . Actually, this ionization does not occur as a single step. The exact mechanisms are not certain, but the complexity can be seen in the twelve step process postulated by Campbell[5] for air.

(A fourth type of collision is called superelastic, and occurs when the electron acquires some of the energy of an excited atom. This de-excitation is often important in gas breakdown, especially with pulsed power, but will not be considered in this paper.)

When the production of electrons in ionizing collisions exceeds electron loss by diffusion, recombination, attachment and wall loss, a condition similar to a chain reaction exists, and breakdown occurs. Most breakdown theory uses the criterion that when the rate of electron production equals the rate of electron loss, breakdown initiates. The difficulty in the theory is finding the appropriate rates for the various mechanisms.

A full explanation of these mechanisms is far beyond the scope of this paper. Numerous books [5,6,7,8,9] deal with the subject in detail, one of the best being MacDonald's [10] This paper will give only a qualitative summary of the processes and indicate the regions where a particular electron loss mechanism is dominant.

COLLISIONS AND ELECTRON PRODUCTION

Integrating the electron acceleration equation 1 gives the velocity

$$2.\quad \text{Velocity} = -\frac{e}{m}\,\frac{Eo}{\omega}\,\cos\,\omega t$$

Note that the velocity expresses the electron flow, or current I. Since the voltage equals Eo sin ωt, the current and voltage are 90° out of phase and the average power gained by the electrons equals zero:

3. Power = VI cos θ

θ = phase angle between current and voltage
cos 90° = 0
V = voltage
I = current

The collisions of electrons with gas molecules give a finite value to cos θ and allow energy transfer from the field to the electrons. This energy transfer is logically dependent upon the collisional frequency νc, which is the number of collisions one electron has in one second. The magnitude of νc depends upon the cross sectional area of the gas molecule, the electron energy, and the particle density of the gas.

Temperature and pressure affect the particle density and hence the collisional frequency as well, as shown by rearranging the gas law:

4. $PV = \frac{N}{No} RT = nRT$

N = number of molecules
No = Avogadro's number 6.02×10^{23} molecules/mole

5. $\frac{N}{V} = \frac{PNo}{RT}$ = Particle density

Thus increasing pressure or decreasing temperature increases collisional frequency. Normally all pressures for gas breakdown are converted to a standard temperature, either 0°C or 20°C.

Assuming νc is independent of electron energy (an assumption that must be used with considerable caution) an average value for air can be expressed as:

6. $\nu_c = 5.3 \times 10^9 \times p$ p in mm Hg @ 20°C.

Obviously the collision rate will interrupt the ordered motion of the electrons as expressed in equation 2. If $\nu_c \gg \omega$, there are many collisions per field oscillation and electron velocities can never reach the maximum. If $\nu_c \ll \omega$, there are many field oscillations per collision and the velocities will approach those expressed by equation 2.

Correcting for collisions, the average electron drift velocity is expressed by [12]:

7. $Vd = \frac{e}{\omega m} Ee$

where $Ee = \left(\frac{Eo^2}{2\left[1 + \frac{\omega^2}{\nu_c^2}\right]} \right)^{\frac{1}{2}} = \frac{E_{rms}}{\left[1 + \frac{\omega^2}{\nu_c^2}\right]^{\frac{1}{2}}}$

The quantity Ee is called the effective field and can be considered the equivalent **d.c.** field for fairly high collision rates. Experimental drift velocities have also been reported [13,14,15].

The relation of ν_c and ω gives a rough idea of the shape and location of the breakdown curves. Breakdown is easiest when the **frequency of the applied electric field** equals the collisional frequency, that is when $\nu_c = \omega$. When ν_c (and pressure as expressed by equation 6) is above or below that point, the average electron energy on collision is reduced and a higher electric field is needed for breakdown. We expect a plot of breakdown electric fields versus pressure to be concave upwards, with the minimum at $\nu_c = \omega$, or expressed differently for air:

8. $p = \frac{2\pi f}{5.3 \times 10^9}$ f in Hertz

However, instead of collisional frequency we need expressions for the ionization rate to balance against electron loss to satisfy the breakdown criterion that rate of electron production equals rate of electron loss. The ionization rate can be related to either collisional frequency νc or drift velocity Vd:

9. $\nu_i = h_i \ \nu_c$ $\qquad h_i =$ probability of ionization

10. $\nu_i = \gamma V$ $\qquad \gamma = \frac{\text{ion pairs produced}}{\text{cm travel}}$

Values for the constants are given in the literature [16,17,18,19,20] and show an energy dependence which further complicates detailed analysis. To get a feel for the numbers involved, an h_i for hydrogen with electron energy of 18 electron volts is given as .01. ν_c for hydrogen is approximately $5.9 \times 10^9 X_p$, so at 1 mm Hg $\nu_i = 5.3 \times 10^9 \times 10^{-2} = 5.3 \times 10^7$ ionizations/sec.

ELECTRON LOSS MECHANISMS

Recombination

If an electron collides with a positive ion, they may recombine to form a neutral molecule. Generally the positive ion concentration before breakdown is too low for the recombination rate to be significant. It may be important, however, in determining decay times for pulsed breakdown. The rate ν_r is given by:

11. $\nu_r = h_r \ \nu_c$ $\qquad h_r =$ probability of recombination per collision

ATTACHMENT

An electron can also attach to a neutral atom or molecule and be lost to the breakdown process. Even though the negative charge of the ion is equal to that of an electron, the mass is so much greater that the drift velocity given by equation 7 is neglibible.

The attachment rate, like the ionization rate, has been related to both collision frequency and drift velocity:

12. $\nu_a = h_a \nu_c$ $\quad h_a$ = efficiency of attachment

13. $\nu_d = \alpha V_d$ $\quad \alpha$ = number of attachments per cm travel

High attachment rates will be observed with molecules whose outer shells are nearly filled, such as chlorine or oxygen. Halogenated fluorocarbons display the same effect. Noble gases with their stable octet have very small attachment rates. The electron affinity energy is a good measure of relative attachment rates of gases for which α or h_a are unknown.

Attachment is important in air breakdown because of oxygen [21,22,23], but is the dominant loss mechanism only at "high" pressures and correspondingly "high" values of ν_c. A pressure is considered "high" when

14. $p\Lambda > 10$ cm-mmHg $\quad \Lambda$ in cm; p in mm Hg

(Λ, the characteristic diffusion length, is a measure of the cavity size and shape and will be discussed in the section on diffusion)

When the inequality 14 holds, there are so many collisions per field oscillation that energy modulation is negligible and $Ee/_p \cong 32$ volts/cm - mm Hg regardless of frequency for air. This determines the right hand side of the breakdown curve.

AMPLITUDE LOSS

When the amplitude of electron oscillation equals the size of the cavity, electrons will be lost to the conductive walls and will not be available for ionization, causing higher breakdown fields. At very "low" pressures, the electrons may strike the walls with sufficient energy to cause re-emission of another electron to the ionization process, thereby lowering the breakdown field. The left end of the breakdown curve is expected, then, to go through a maximum and decrease again at very low pressures.

Theoretical calculations of when amplitude loss becomes dominant is difficult [10], but empirically it would be expected at an inflection point in the curve or when the first derivative of the curve equals zero. Because of the large cavities employed in commercial freeze drying, amplitude loss usually will not be dominant in the normal pressure range of freeze drying.

DIFFUSION:

Since attachment is dominant at "high" pressures and amplitude loss is dominant at "low" pressures, diffusion is said to dominate the "middle" range of pressure, which is the region of interest for freeze drying (around 1 mm Hg). Diffusion of electrons should be visualized as a movement superimposed on the electron oscillations caused by the electric field. If the centers of oscillation are traced, they will move in the direction of decreasing electron concentration (the walls).

If we take the electron concentration as

$$15.\quad n_e = \frac{Ne}{Vol}$$

Ne = number of electrons
Vol= volume, cm^3,

then the driving force of diffusion is the gradient of electron concentration

$$16.\quad \nabla n_e = \frac{\partial ne}{\partial x} + \frac{\partial ne}{\partial y} + \frac{\partial ne}{\partial z}$$

The flow of electrons by diffusion is expressed then by Fick's Law:

$$17.\quad \frac{Q}{A} = -\nabla D n_e$$

Q = number of electrons/sec.
A = cross sectional area for electron flux
D = diffusion constant

Note that equation 17 is similar to the heat conduction formula

$$18.\quad \frac{q}{A} = -k \frac{dt}{dx}$$

q = Btu/hour
A = area for heat flux
k = constant of thermal conductivity
dt/dx = temp. gradient

The difference is that heat conduction is energy transfer and diffusion is mass transfer.

The rate of change of electron concentration by diffusion then becomes

$$19.\quad \frac{\partial ne}{\partial t} = \nabla^2 (Dne)$$

or for D independent of spatial variation

$$20.\quad \frac{\partial ne}{\partial t} = D\nabla^2 n_e$$

Continuity Equation (Electron balance)

Using the criterion for breakdown that the electron production rate equals the sum of the loss rates, we can combine equations 9, 12 and 20 to give

$$21.\quad \frac{\partial ne}{\partial t} = \nu_i n_e - \nu_a n_e - D\nabla^2 n_e \overset{6,10}{=} 0.$$

ν_i and ν_a have the n_e term because they are both rates for a single electron. Rewriting 21 we get

$$22. \quad (\nu_i - \nu_a) n_e = D \nabla^2 n_e$$

Unfortunately, the values of D for electrons moving in high electric fields are not generally known. Theoretical calculations of D depend on electric field, pressure, and the electron velocity distribution function (the average drift velocity Vd is not sufficient). MacDonald[10] has treated this problem, but less detailed analysis makes the assumption of the ionization rate ν_i being independent of spatial variation (i.e., the electric field is uniform throughout the region of interest).

With this assumption, both sides of 22 may be set equal to a constant $-\gamma$ such that

$$23. \quad \nabla^2 n_e = -\frac{\gamma n_e}{D}$$

The value of γ/D depends upon the size and geometry of the cavity. Brown[7] and MacDonald[10] give the following relations for different geometries:

For right cylindrical cavity with conductive walls:

$$24. \quad \gamma/D = \left(\frac{2.405}{R}\right)^2 + \left(\frac{\pi}{X}\right)^2$$

R = radius of cylinder
X = height of cylinder

For rectangular parallelepipeds in the dominant mode:

$$25. \quad \gamma/D = \pi^2/X^2 + \pi^2/Y^2 + \pi^2/Z^2$$

X, Y, Z dimensions of sides

Because γ/D has units of cm^{-2} a <u>characteristic diffusion length</u>, Λ, is defined such that

26. $\gamma/D = 1/\Lambda^2$

For the case of infinite parallel plates, the diffusion length is simply

27. $\Lambda = d/\pi$ d = plate separation, cm

Most microwave breakdown work has been done with Λ a fraction of a centimeter or a couple of centimeters at most, in cavities designed for a single mode, most often the $TE_{01\,0}$[24]. But the general case for an industrial freeze drier is a large multimode cavity with a geometric Λ much larger. However, with a multimode cavity the assumption of uniform electric field implicit in equations 24, 25 and 26 no longer holds.

The true Λ is much smaller than the geometry indicates, because if electrons move from a high electric field region to a lower one they are as effectively lost to breakdown as if they diffused to the walls. The electric field density as expressed by the dominant mode of the cavity is also important in that it affects the assumption of ν_i being independent of spatial variation[26].

Λ for large cavities cannot normally exceed one wavelength of the applied field[10], since this represents the maximum periodic spatial variation of the electric field. The large-cavity-Λ can be much smaller if localized high intensity fields exist. Such localized fields cause a sphere or ovoid of breakdown, the so called "glowball", and the approximate diffusion length is given by

28. $\Lambda = r/\pi$ r = radius of "glowball"

Sharp points or discontinuities in the microwave freeze dry cavity will cause such localized fields and must be avoided, both to minimize breakdown and to ensure even dielectric heating of the food.

We have already discussed the effects of temperature and pressure and are now in a position to qualitatively understand the effects of frequency, gas composition, and cavity size and shape upon breakdown curves.

GAS COMPOSITION

We expect different gases to have differing breakdown curves. A high ionization potential gas requires high energies and correspondingly high electric fields for breakdown, while a gas like neon requires relatively low fields. A gas with a high electron affinity energy such as chlorine or freon should have a high attachment coefficient and also require high fields, while gases like argon should require low fields. A gas with a large collisional cross sectional area should have a relatively high collisional frequency ν_c, and the minimum breakdown should occur at relatively lower pressures, as shown by equation 8.

Figure 2 illustrates these points, and Table 1 gives some applicable physical constants.

Table 1 - Selected Constants of Gases

Gas	Molecular diameter-viscosity[26]	Effective collision Molec. Dia.	First lonization Potential
O_2	2.96 Å	4.3 Å	12.1 e.v.
N_2	3.16 Å	5.5 Å	15.6 e.v.
H_2	2.18 Å	3.1 Å	15.44 e.v.
A_r	2.86 Å	3.7 Å	15.77 e.v.
CO_2	4.60 Å	7.6 Å	--------

Bleeding in a gas with higher breakdown strength than air is one method of increasing the allowable electric field for microwave freeze drying. Note that a gas may have a breakdown field higher than a second gas in one pressure region and lower in another region. Care must be taken to do comparisons in the pressure range of interest.

Unfortunately breakdown curves are not known for very many gases. A large part of the literature concerns itself with low breakdown strength noble gases because of the good agreement between theory and experiment. Even very sophisticated theory fails in predicting breakdown curves for polyatomic molecules because of computational difficulties in establishing the electron velocity-energy distribution function, and because of the lack of accurate physical constants (h_a, h_i, h_r, ν_c, etc.). Thus a realistic approach to choosing a bleed-in gas would be trial and error, guided by the qualitative principles stated above.

FREQUENCY

Since the minimum in the breakdown curve occurs approximately where $\omega = \nu_c$, we expect the curve to shift to the right for higher frequencies. A second result of higher frequencies is an upward shift of the curve, because of the shorter half cycle time for acceleration of the electrons. Recalling the velocity equation

$$2. \quad \text{Velocity} = \frac{e}{m} \frac{Eo}{\omega} \cos \omega t$$

we see that increasing the frequency ω decreases the magnitude of velocity and energy modulation, thereby decreasing the rate of electron production. Figure 3 shows the curve shift due to frequency.

Working at higher frequencies would yield a double advantage of higher breakdown fields and greater heating of the dielectric according to the familiar power equation.

$$29. \quad P = 8.85 \times 10^{-14} \quad 2\pi f \epsilon''_r E^2$$

P = power watts/ cm^3

E = electric field volts/cm

ϵ''_r = relative loss factor

f = frequency Hertz

Higher frequencies do have the drawback of smaller half depth penetration; but for the case of frozen foods as in freeze drying, the penetration at 2450 MHZ. is still deep enough to assume as good volumetric heating as at 915[26] MHZ.

The loss factor ϵ''_r is also a function of frequency, but for most foods the factor $f\epsilon''_r$ increases for increasing frequency [28], so the power absorption is still increased or remains constant without changing the electric field. When we also square the allowable breakdown fields shown in figure 11 for air at 915 and 2450 MHZ and insert into equation 29, the advantages of higher frequencies become apparent.

The conclusions of various researchers working at 915 MHZ. that very low operating pressures are needed [12] and that the economics of microwave freeze drying are unfavorable [28] do not necessarily hold at 2450 MHZ, the other common ISM frequency for food processing. For example, at 1 mm Hg and for $\lambda \approx 3$ cm) the breakdown field for 2450 MHZ is about 230 volts/cm and for 915 about 100 volts/cm. The ratio of maximum power absorption without breakdown is therefore:

$$30. \quad \frac{P\ 2450}{P\ 915} = \left(\frac{2450\ MHZ}{915\ MHZ}\right)\left(\frac{\epsilon''r\ 2450}{\epsilon''r\ 915}\right)\frac{(E\ breakdown\ 2450)^2}{(E\ breakdown\ 915)^2}$$

Taking representative ϵ''_r for ground beef for 1,000 and 3,000 MHZ [29], the ratio $\frac{P\ 2450}{P\ 915}$ approximately equals 5.3.

Clearly frequency has a strong effect on economics, and 2450 MHZ may be more suitable than 915 MHZ for freeze drying.

Effect of Cavity Size

For a given frequency and gas, we expect the minimums of the curves for different diffusion lengths (Λ) to fall at about the same pressure. The electric fields for "high" pressures are the same, since for $P\Lambda > 10$ attachment is the dominant loss mechanism and breakdown fields are relatively independent of cavity size. At "low" pressures where the amplitude of oscillation can reach its maximum (because for $\nu c \ll \omega$ there are many field oscillations per collision) we expect lower breakdown fields for a larger Λ. All this means is that for a larger Λ there is a larger region of uniform intense field to give greater acceleration and energy to the electrons, and that the cavity is larger and can contain these larger oscillations without amplitude loss to the walls. Figure 4 shows these effects.

As Λ increases beyond one centimeter, the differences in the curves become less pronounced. This is helpful because for large cavities Λ will be large and difficult to determine precisely from estimation of the radius of the "glowball". An alternate method is to estimate the point where the breakdown curve becomes linear and assume $\Lambda = 10/p$. Both methods are crude but usable when a geometric Λ fails.

Summary Simplified Breakdown Theory

If νc was independent of electron energy, all breakdown data for a gas could be presented on a two dimensional graph using the lumped parameters Ee Λ vs. p Λ, as in Figure 5. (Remember that Ee includes a frequency term, so that electric field, frequency, pressure, and cavity size are all represented.) Figure 5 works very well for the conditions of p $\Lambda > 10$, when Ee/p = 32 and for p $\lambda > 100$, when Ee = E and breakdown becomes independent of frequency. At lower values of p Λ the assumptions no longer hold and νc becomes energy dependent. A more complex semi-empirical system by MacDonald [10] relates all available breakdown data for air. Again, the theory does not apply to breakdown in other gases and must be used cautiously in predicting freeze-dry breakdown fields because of the water vapor partial pressure.

Lastly, none of the literature theory or experiment allows for a dielectric load in the cavity. The author's work in this paper will therefore derive and test expressions for the effects of cavity loading on breakdown fields. Also, no-load curves for air, water vapor, and CO_2 for 2450 MHZ as determined by the author in a multimode cavity will be presented and compared with the qualitative principles mentioned before.

Experimental Work

Apparatus

2450 MHz was used for all of the present work because of the assignment of this frequency to I.S.M. use, and the availability and common use of 2450 MHZ sources for food processing. Figure 6 shows the equipment in block form.

The source A is an Amperex DX-206 1 KW magnetron. It is connected via 1 5/8-inch coax B to a waveguide circulator C which shunts the reflected

power to a dummy load D preventing reflection to the source. An H-tuner E varies the admittance of a second dummy load F to the forward power, giving variable attenuation. A bidirectional coupler G samples forward and reflected power, and a switch H sends one or the other RF signal to a rectifier I which gives a voltage output for display on an oscilloscope J.

A waveguide switch K directs the forward power to either the cavity O or a water load L. A thermopile M gives a voltage proportional to the temperature rise in the water load, which is read on a millivoltmeter N. Figure 7 shows the overall equipment set up.

An antenna beams the power into the cavity. The vacuum system is a Pyrex flask P placed within the cavity, with gas bleed-in from the sources R controlled by needle valves in series Q. A Stokes-McLeod gauge S reads pressures of 0-5mm and a Wallace and Tiernan diaphragm gauge T reads pressures of 0-100 mm. A vapor trap U cooled by dry ice and ethanol prevented water contamination of the vacuum pump V during water breakdown runs. Figure 8 shows the vacuum flask-cavity set up.

The equipment used has limitations. First, as noted by Towne 29 a magnetron is a rather noisy source when speaking of spectroscopy or breakdown, and most of the literature work was done with ultrastable monochromatic sources. A noise source can have lower breakdown fields than a pure source, but only if $\Delta\omega \gtrsim \omega_o$. For commercial sources of 2450 MHZ + 50 MHZ, this effect can be ignored.

A second equipment limitation is that with constant bleed-in of gas, breakdown occurs in a gas flow rather than under the static conditions of most literature work. Freeze drying of course, involves gas flow, and the author wished to investigate the effects. Skinner and Brady [30] related flow effects to the critical velocity of the gas while duplicate runs by the author with flow

and stagnant gas showed no significant difference. Care must be taken in static breakdown however, so that all the products of the plasma are removed and fresh gas added before the next run. Failure to do this can give breakdown fields up to 10% too low[31].

Another source of error was temperature and composition control. Air was no problem since dessicated ambient air was used. The vacuum boiled distilled water used as a water vapor source had dissolved gases that had to be distilled off, and small air leaks in the system contaminated both the water and carbon dioxide runs. The temperatures of water and CO_2 gas were below ambient at the sources and were warmed by conductive-convective heating through long lead-in tubes to the cavity, but this method is far from precise. Thus while the air breakdown curves are quantitative, the other two should be considered as giving qualitative breakdown relative to air.

A final equipment limitation is that the magnetron power supply used in the author's work is a full wave rectifier type which gives pulsed rf output at twice the line frequency (i.e., 2 x 60 HZ = 120 pulses/sec). The breakdown fields for pulsed rf are greater than for CW, a nd Copson[32] has suggested pulsed power as a way to increase the electric field and dielectric heating in microwave freeze drying.

The breakdown fields for pulsed rf are greater than those for CW because there are fewer collisions in which the electron can acquire ionization energy. The energy acquired in one pulse is degraded by elastic collisions before the next pulse occurs, so the electron chain reaction must initiate in a single pulse. The theoretical approach to pulsed breakdown is difficult because the continuity equation must be solved for transient rather than steady states.

The experimental work on pulsed breakdown has been summarized by MacDonald[10] as in figure 9, which uses the ratio of (E pulsed breakdown field/ECW breakdown field)

as a function of cycles per pulse, allowing comparison of different frequencies and pulse lengths. As might be expected, long pulses give values approximating CW.

Recalling that absorbed power is proportional to the electric field squared and correcting for the finite time between pulses when power absorption equals zero, we can write

$$31. \quad \frac{P \text{ pulse}}{P_{cw}} = \frac{(Eprms)^2}{(Ecwrms)^2} \quad \frac{tp}{Tp} = \frac{(Eprms)^2}{(Ecwrms)^2} \quad (tp) \quad (fp)$$

Where tp = pulse time per cycle with non zero power.

$$Tp = \text{total pulse time peak to peak} = \frac{1}{\text{pulse repetition rate}}$$

$$= 1/fp$$

Therefore for pulsed power to be an advantage, the quantity (P pulse/P cw) of equation 31 must be greater than unity. For the author's work tp/Tp = 0.743 (determined from oscilloscope display of forward power pulses.) Taking that portion of the pulse within 10% of the peak voltage, there are 3.76×10^6 cycles/pulse, giving $E_p/E_{cw} = 1.04$, and a ratio P_p/Pcw of 0.804. Much shorter pulse lengths are thus needed to make pulsing advantageous. For example, with 1 μ sec pulses at 2450 MHZ, 250,000 pulse/sec would be necessary just for P_p to equal Pcw. Normal pulse units do not go over 100,000 pulses/sec, and the cost of microwave sources with higher pulse rates and the large duty cycles involved would tend to offset any increase in absorbed power. Pulsing does not seem to be the answer.

Determining Electric Field Strength

We still need a method of relating power to the electric field strength. Most literature work measures the VSWR on resonance, the cavity Q and the incident

power at the instant of breakdown. This method though, is only applicable to empty cavities operating in a single dominant mode. The author derived instead a less precise but more general form involving absorbed power allowing for loads. Since forward and reflected power can be measured by a bidirectional coupler or power meter, assuming negligible VSWR between the detector and the cavity we can write

32. Power in - Power out = Power absorbed in cavity

33. P absorbed = P skin loss + P dielectric loading loss

Since the skin loss is analogous to a resistance loss in an LC circuit, we postulate a form for the first loss of

34. P skin loss = KE^2 where $K = \frac{1}{\text{resistance}}$ = admittance

The value of K can be determined for an unknown cavity by measuring P in and P out for the empty cavity for a known breakdown field. For an arbitrary multimode cavity, Λ will not be known, so an arbitrarily high pressure is used to make $p\Lambda > 10$, giving $Ee/p = 32$ volts/cm mm Hg. If $p\lambda > 100$, the breakdown also becomes independent of frequency and available literature curves for other frequencies may be used directly.

Rearranging equation 34., K is simply

35. $K = \frac{P_{in} - P_{out}}{E^2}$

For a cavity not yet built, a reasonable value of K can be calculated from

36. $E_o = \sqrt{\frac{P_o Q_u}{\eta \omega_o}}$ or $P_o = E_o^2 \frac{\eta \omega_o}{Q_u} = KE^2$

Which means that

$$37. \quad K = \frac{\eta \omega_o}{Qu}$$

Where: ω_o = resonant freq., radians/sec

P_o = power absorbed at resonance, watts

$Qu = 2\pi \frac{\text{energy stored in cavity}}{\text{energy lost in cavity}}$

$$38. \quad \eta = b\, \epsilon_o\, V$$

b = constant of electric field distribution

ϵ_o = free space permittivity 8.84×10^{14} farad/cm

V = volume of cavity cm^3

The theoretical Qu is given by Harvey [33] for various dominant modes. Assuming a $T E_{202}$ mode (a reasonable set of eigen values for the author's cavity), we get

$$39. \quad \frac{Qu\delta s}{} = \frac{ABC}{2} \quad \frac{[(1/A)^2 + (n/c)^2]^{3/2}}{(1/A)^2\, C\, (A+2B) + \left(\frac{n}{c}\right)^2 C + 2B}$$

Where: m, n, l, are eigenvalues of $T E_{m n}$

A, B, C are dimensions of cavity A=B=C=24.5cm

δs = skin depth.

λ = free space wavelength = 12.25 cm

Substituting appropriate values in 37, 38 and 39 and taking $b = (0.707)^2$ for the average electric field squared for half sinusoidal distribution, we get a theoretical K of 0.37×10^{-3} versus an empirical K of 0.39×10^{-3} determined by equation 37.

This is a very close correlation, considering the exact δs of the cavity was not known and that only the dominant cavity mode was considered. The theoretical method should give reasonable values of skin loss for theoretical design of microwave freeze dry cavities.

Large cavities have a real advantage in reducing skin loss, since Qu is roughly proportional to the volume divided by the surface area. Taking our cubic cavity of side X, the volume equals X^3 and the area equals $6\ X^2$. Thus Qu increases with X as

$$40. \qquad \frac{X^3}{6\ X^2} = \frac{X}{6}$$

and the large Qu's associated with larger X's give smaller K's according to equation 37, and correspondingly smaller skin losses for a given electric field by equation 34.

As for the dielectric loss, we refer again to the power equation 29.

$$41. \qquad P = 2\ \pi\ f\ \varepsilon''\ r\ \ 8.85 \times 10^{-14}\ \ E_d{}^2\ \text{Volume dielectric}$$

Note that we want total watts loss, so we have multiplied 29 by the volume of dielectric. We have also introduced a subscript E_d, because the field inside the dielectric is <u>less</u> than the free space electric field Ef by

$$42. \qquad Ed = \frac{Ef}{\sqrt{(\varepsilon''_r)^2 + (\varepsilon'_r)^2}}$$

We must keep clearly in mind that the breakdown and skin loss are determined by Ef and the dielectric heating by Ed, all expressed as rms values. Also, 41. must be corrected for pulsing. Combining 31., 41. and 42. we get

$$43.\quad P = \frac{2\pi f \epsilon''_r\, 8.85\times10^{-14} (Ef_p)^2 \text{ Vol. Diel.}}{(\epsilon''_r)^2 + (\epsilon'_r)^2} \qquad \frac{tp}{Tp}$$

Where Ef_p refers to the rms of the pulse alone, since the term $\frac{tp}{Tp}$ corrects for the zero power portion of the cycle. Combining 35, 41, and 42 we get for CW input to a cavity with n dielectric loads

$$44.\quad Efcw = \sqrt{\frac{P_{in} - P_{out}}{K + \sum_{i=1}^{n} \frac{2\pi f \epsilon''_{ri}\, 8.85\times10^{-14} \text{Vol. diel.}_i}{(\epsilon''_{ri})^2 + (\epsilon'_{ri})^2}}}$$

or simply $Efcw = \sqrt{\frac{P_{in} - P_{out}}{K + C_1 + C_2 + \ldots Cn}}$

For pulsing, the rms of the pulse alone (which determines breakdown) is given by

$$45.\quad Ef_p = \sqrt{\frac{P_{in} - P_{out}}{(K + C_1 + C_2 + \ldots Cn)} \left(\frac{tp}{Tp}\right)}$$

The resulting values of Ef_p for the author's work were converted to an equivalent Ef_{cw} via Figure 9 for plotting and comparison with theory.

EVALUATION OF CONSTANTS.

C_1 in equation 45 represents the Pyrex vacuum system within the cavity. Because of the power limits of the equipment, no breakdown could be initiated at atmospheric pressure and this meant that K could not be independently determined. Instead, C and K were lumped and the sum was found empirically to equal 1.65×10^{-3} (corrected for pulsing). C equals 1.26×10^{-3} from equation 4 ., giving a K of 0.39×10^{-3} by subtraction, versus a theoretical K of 0.37×10^{-3} by equations 37, 38 and 39 as stated previously. Thus we

have an expression for E as a function of measured power and some constants. The power is read simply by couplers or meters, and once the constants K, C_1, C_2, ...Cn are known a simple slide rule calculation is all that is needed.

The (P in - P out) term was found by multiplying calorimetrically measured forward power by 1 -(Power reflected/Power forward).

The ratio (P refl/ P for) is found from the oscilloscope display of rectified rf from the bidirectional coupler as

$$46. \quad \frac{P_{refl}}{P_{for}} = \frac{(\text{Voltage reflected})^2}{(\text{Voltage forward})^2}$$

The voltage readings are taken just before breakdown, because the corona increases power absorption. Figure 10 shows characteristic oscilloscope traces of rf power sampled by the bidirectional coupler. 10a shows forward power and 10b shows the relative reflected power (about 25%) from the cavity containing the Pyrex vacuum system. 10c shows the reflected power during gas breakdown (not on same scale as 10a and 10b - the breakdown reduces reflected power).

The actual breakdown points were determined by holding either pressure or power constant and varying the other until a glow was visible in the cavity. The vacuum system was flushed after each breakdown and allowed to cool again to ambient temperature (besides dielectric heating of the Pyrex, the glowball can cause intense heating by conduction-convection).

Λ was estimated by two methods:

(1) When $p\Lambda > 10$, the curve of log E vs log P becomes linear, and $Ee/p = 32$. Thus $\Lambda = 10/p = 0.67$ cm

(2) The diameter of the smallest possible "glowball" is about one inch. Thus from equation

$$28. \quad \Lambda = r/\pi = {}^{2.54\ \text{cm}}/_{3.14} = 0.81\ \text{cm}.$$

The value of Λ from (1) is considered more accurate by the author and was used for the theoretical curves of Figure 11 derived from the simplified breakdown theory of MacDonald. (Fig. 5).

Comparison of Experiment and Theory

Figure 11 shows the experimental breakdown curve for air at 2450 MHz and theoretical curves for air at 915 MHZ and 2450 MHz. Figure 12 shows the experimental breakdown curves for air, water and CO_2 .

Note that the optimum breakdown for air occurs approximately where $\omega = \nu c$ ($2\pi f = 5.3 \times 10^9 p$, or $p = 2.95$ mm) and that the theory works well for "high" pressures where the assumptions of the derivation holds.

At "low" pressure where $\nu c \ll \omega$ the assumption of a homogeneous electric field no longer holds, and higher electric fields are needed than theory predicts as the electrons are swept out of the intense field region. At the inflection points of the left ends of the curves of Fig 11 & 12 the oscillation amplitude approximates the geometric Λ which is larger than the Λ representing the intense field region. As the pressure decreases below the inflection point, the experimental breakdown fields become smaller than theory predicts, as re-emission from the walls becomes more pronounced. Below about 100 microns pressure the experimental breakdown fields actually decrease again.

This decrease at "low" pressures may be very important near the end of the freeze dry cycle when the constants Cn for the food are small and the pressure is also very low. Bleeding in a high breakdown strength gas and/or raising the pressure may have great advantages during this final stage, but a tradeoff must be made between the pressure gradient for mass flow and the maximum dielectric heating determined by the breakdown fields. Fortunately the mass flow for the last stage is diffusive, which depends upon the partial pressure of water vapor rather than total pressure. Thus a higher pressure of a second or third gas should not limit the mass flow until the transition to laminar flow. Note in Figure 12 that water vapor is a gas which has higher breakdown fields than air above 2 mm Hg but lower than air below that pressure. The higher region is caused by the high recombination rate of water vapor (recall that recombination becomes dominant at "high" pressures). The low pressure difference can be attributed to a low collision frequency νc.

The agreement of the theoretical and experimental curves in Figure 11 is also a check upon the validity of equation 45, which was used to determine experimental values of E from power measurements.

A final test of equation 45 was made by placing a second dielectric load C_2 in the cavity. The block of plexiglass used had a loss factor of .0166, about the same as frozen beef, and a C of 0.58×10^{-3}. Referring to equation 45, we see that more power is needed for breakdown at a given pressure. As a check on the effect of the plexiglass block reducing the volume of the Pyrex flask and possibly affecting A, a block of low-loss polyethylene of equivalent volume was also tested. C for the polyethylene was $.0027 \times 10^{-3}$, which is neglibible in comparison to $K + C_1 = 1.65 \times 10^{-3}$. Table 2 summarizes these results which show agreement between theory and experiment within the limits of experimental error.

Table 2 - Effect of Plexiglass and Polyethylene dielectric Loads on Breakdown Fields

Dielectric Material	Power (watts)	$\frac{(V\text{reflected})^2}{(V\text{forward})^2}$	Ef theory Eq.47 volts/cm	Ef actual volts/cm	E_{th}/E_{act}
Plexiglass	230	77%	300	302	.995
$\epsilon'_r = 2.60$	188	75%	267	260	1.03
$\epsilon''_r = .0064$	155	75%	243	232	1.05
interpolated between 1000 MHZ & 3000 MHZ at 25°C.	128	75%	221	212	1.04
Polyethylene	230	75%	339	338	1.00
$\epsilon''_r = 4 \times 10^{-4}$	188	75%	307	309	.99
$\epsilon'_r = 2.26$	155	78%	279	284	.98
	128	75%	253	272	.93
	110	75%	235	232	1.01

SUMMARY

A method has been derived and tested for determining absolute electric field strengths and approximate breakdown fields for the general case of freeze drying with microwaves. The parameters of frequency, cavity shape and size, pressure, temperature, and dielectric load were included in the analysis. The frequency has a strong effect on the economics of microwave freeze drying and 2450 MHZ appears better than 915 MHZ from a theoretical standpoint. The use of pulsing to avoid breakdown is not practical because of the reduced power absorption. For precise prediction of maximum power input without breakdown throughout a freeze-dry cycle, the gas temperature, pressure and composition must be known, along with sublimation rates and dielectric constants and loss factors for the food. The effect of the partial pressure of water vapor is important and more work needs to be done on breakdown in mixtures of air and water vapor. Future work should also relate the sublimation rate to the theoretical heating rate which is easily obtainable from equation 44 or 45 in conjunction with the power equation 41 and 42. Lastly, future work should test the derivations for food dielectric loads throughout freeze drying cycles.

This methodology can be applied to any other microwave heating application as well for determining electric field strengths and theoretical heating rates. The value of K can be calculated theoretically by equation 37, 38 and 39, (Note that 39 refers only to a TE_{202} mode - see the reference 21 for others) or by experiment. In the latter case, operating at a pressure high enough such that $p\Lambda > 10$ and $p\lambda > 100$, the absolute values of the field are simply $Ee/p = 32$ volts/cm-mm Hg and K can be easily determined from equation 35.

While electric field strengths can be determined more accurately by other methods for waveguides and small cavities, this method is suitable for large multi-mode cavities. The main advantage of the breakdown method over bolometers, etc. is that the electric field is not disturbed by a detector.

Also, the use of coronas may be useful in design and testing of cavities. A cavity-contained corona gives a direct display of relative field intensities, identifying hot spots and modes (see Fig. 1). This use was first suggested by the Amperex Co. in one of their technical reports[35], but it explained no means of quantitative measurements.

A final note on the accuracy of the author's method: a homogeneous electric field was assumed throughout the cavity for determining power losses. While this is not a true assumption for point to point power absorption, taking the total cavity absorption assumes that the maximum and minimum electric field average out to the same effect as an average even field throughout the cavity. This assumption proved to be good, at least for the cavity used in this work, and should hold for any well designed cavity with a load large enough to occupy both maxima and minima in the electric field. For applications to freeze drying, we should also keep in mind that the inaccuracies due to measured ϵ''_r and ϵ'_r for foods are probably greater than the errors due to assumptions involved in the author's derivations.

Lastly, as described by Copson[33], the dielectric heating of a Pyrex vacuum system within the cavity like that used in this work contributes significant radiative heating for longer cycle times. This makes such a setup unsuitable for freeze drying, and the recommended alternative is to place the cavity inside a larger vacuum chamber as Hoover et al [1,2] did or by making the chamber itself serve as the vacuum container.

REFERENCES

1. Hoover, M.W., Markanonatos, A., Parker, W.N.; "Experimental Accelerated Freeze-drying of foods by means of UHF dielectric heating"; Food Technology 20: 807-14 June 1966

2. Hoover et al, "Engineering Aspect of Using UHF Dielectric heating to accelebate the Freeze Drying of Foods" Food Technology 20:807-14 Jun 66

3. Copson, David A., Microwave Heating, AVI publishing Co., Westport Conn. 1962

4. Cotson, S., Smith, D.B/, Freeze drying of Foodstuffs, Columbine Press, London 1963

5. Campbell, Ali Bulent, Plasma Physics and Magneto fluid mechanics, McGraw H Hill, N.Y. 1963.

6. Francis, G., Ionization Phenomenon in Gases, Academic Press., N.Y., 1963

7. Brown, S.C., Introduction to Electrical Discharge in Gases, John Wiley & Sons, Inc., New York 1966

8. Brown, S.C., Basic Data of Plasma Physics, MIT Press, Cambridge MA, 1966

9. Brown, S.C., Molecular Science & Molecular Engineering, John Wiley & Sons Inc., N.Y. 1959

10. MacDonald, A.D., Microwave Breakdown in Gases, John Wiley & Sons, N.Y. 1966

11. Gould, L., Roberts, L.W., "Breakdown of air at Microwave Frequencies", Journal of Applied Physics Vol. 27 #10 October 1956

12. Brown, S.C., Basic Data of Plasma Physics, MIT Press, Cambridge, MA., 1966

13. Nielsen, R.A., Bradbury, N.E., Physics Review., J1 V51 P. 69.

14. Ryzko, H., Phypro J3 V85 P.1283 1965

15. Pack, J.L., Voshall, R.E., Phelps, W.V., Phyrev J 1 V127 P. 2084 1962

16. Harrison, M/A., Phyrev J1 V105 P.366 1957

17. Golden, D.E., Fisher, L.H., Phyrev J1 V123 P.1079 1961

18. Freely, J.B., Fisher, L.H., Phyrev J1 V133 P. 304 1964

19. Chanh, L.M., Rork, G.D., Phyapp J11, V36 P.155 1965

20. Dutton, J, Harris, F.M. Jones, F.L., Phypro J3 V81 P.52 1963

References (continued)

21. Chann, L.M., Phelps, A.V., Biondi, M.A., Physics Review VI V128 P. 219 1962

22. Burch, D.S., Geballe, R., Physics Review J1 V106 P. 183 1957

23. Bradbury, N.E., Physics Review V.44 P.885 1933

24. Self, S.A., Boot, H.A. "The Effect of Field Configuration on Gas Discharge Breakdown in Microwave Cavities at Low Pressure", J. Elec. & Control. Vol 6 No. 6 pp. 527-47 Jun 1959.

25. Moore, W.J., Physical Chemistry, Prentice Hall Inc., Englewood Cliffs, N.J. 1962

26. Copson, David A., "Microwave Sublimation of Foods", Food Technology, P_p 270-2 Jun 58

27. Grimm, A.C., "A Technical and Economic Appraisal of the Use of Microwave Energy in the Freeze-Drying Process" ST - 3980, RCA Review, Dec. 1969

28. Van Dyke, D., "Dielectric Parameters of Ground Beef and their Correlation with Pertinent Variables", Master's Thesis MIT, 1968

29. Townes & Schawlow, Microwave Spectroscopy, McGraw Hill, N.Y., P. 405 1955

30. Skinner, J.G., Brady, JJ., "Effect of Gas Flow on the Microwave Dielectric Breakdown of O_2", J., Applied Physics (USA) Vol 34 No. 4 I, P_p 975-8, Apr 1963

31. Rose, D.J., Brown, S.C., J. Applied Physics, 28 P 561 1957

32. Copson, D.A., Microwave Heating, AUI Publishing Co., Inc., Westport, Conn, p. 163 1962

33. Harvey, A.F., Microwave Power Engineering, Academic Press, N.Y. P. 194 1963

34. Piaser, B., "Microwave Oven Coupling Procedures", Engineering and Laboratory Report No. 468 Amperex Electronic Corporation, Hicksville, N.Y. Dec 1964

LIST OF SYMBOLS

A	cross sectional area	cm^2
a	acceleration	cm/sec^2
b	constant of electric field distribution	dimensionless
D	electron diffusion coefficient	$cm\ sec^{-1}$
$E \equiv E_{rms}$	root mean square of electric field	volts/cm
E_e	effective electric field	volts/cm
E_o	maximum electric field	volts/cm
e	electron charge	coulombs
f	field frequency	Hertz
fp	pulse repetition rate	pulses/sec
h_a	efficiency of attachment	attachments/collision
h_i	probability of ionization	ionizations/collision
h_r	probability of recombination	recombinations/collision
I	current	amperes
K	admittance of cavity	ohm^{-1}
k	thermal conductivity	$\frac{Btu\text{-}ft}{hr\text{-}ft^2\text{°}F}$
m	electron rest mass	grams
N	number of molecules	
Ne	number of electrons	
N_o	Avogadro's number	6.02×10^{23} molecules/mole
α	attachment coefficient	attachments/cm travel
γ	ionization coefficient	ion pairs produced/cm travel
	constant equal to	D/Λ^2
∇	differential operator	$\partial/\partial x + \partial/\partial y + \partial/\partial z$
δ_s	half power skin depth	cm
ϵ_o	free space permittivity	8.84×10^{-14} farad/cm
ϵ_r'	relative dielectric constant	
ϵ_r''	relative loss factor	
θ	phase angle between current and voltage	radian
Λ	characteristic diffusion length	cm
λ	free space wavelength of applied field	
ν_a	attachment frequency of one electron	attachments/sec
ν_c	collisional frequency of one electron	collisions/sec
ν_i	ionization frequency of one electron	ionizations/sec
ν_r	recombination rate of one electron	recombinations/sec
ω	applied field frequency	radians/sec
ω_o	resonant frequency	radians/sec

n_e electron concentration electrons/cm^3

P power absorbed watts/cm^3

P_o power absorbed at resonance watts

p pressure mm Hg

Q electron flux electrons/sec

Qu $2\pi \frac{\text{energy stored in cavity}}{\text{energy lost in cavity}}$

q heat flux Btu/hr

R gas constant

r radius cm

Tp total pulse cycle time sec peak to peak

t time sec

tp pulse time per cycle sec with non-zero power

V volume cm^3

V_d electron drift velocity cm/sec

X,Y,Z dimensions of rectangular parallel piped cm

Subscripts p = pulsed
cw = continuous wave

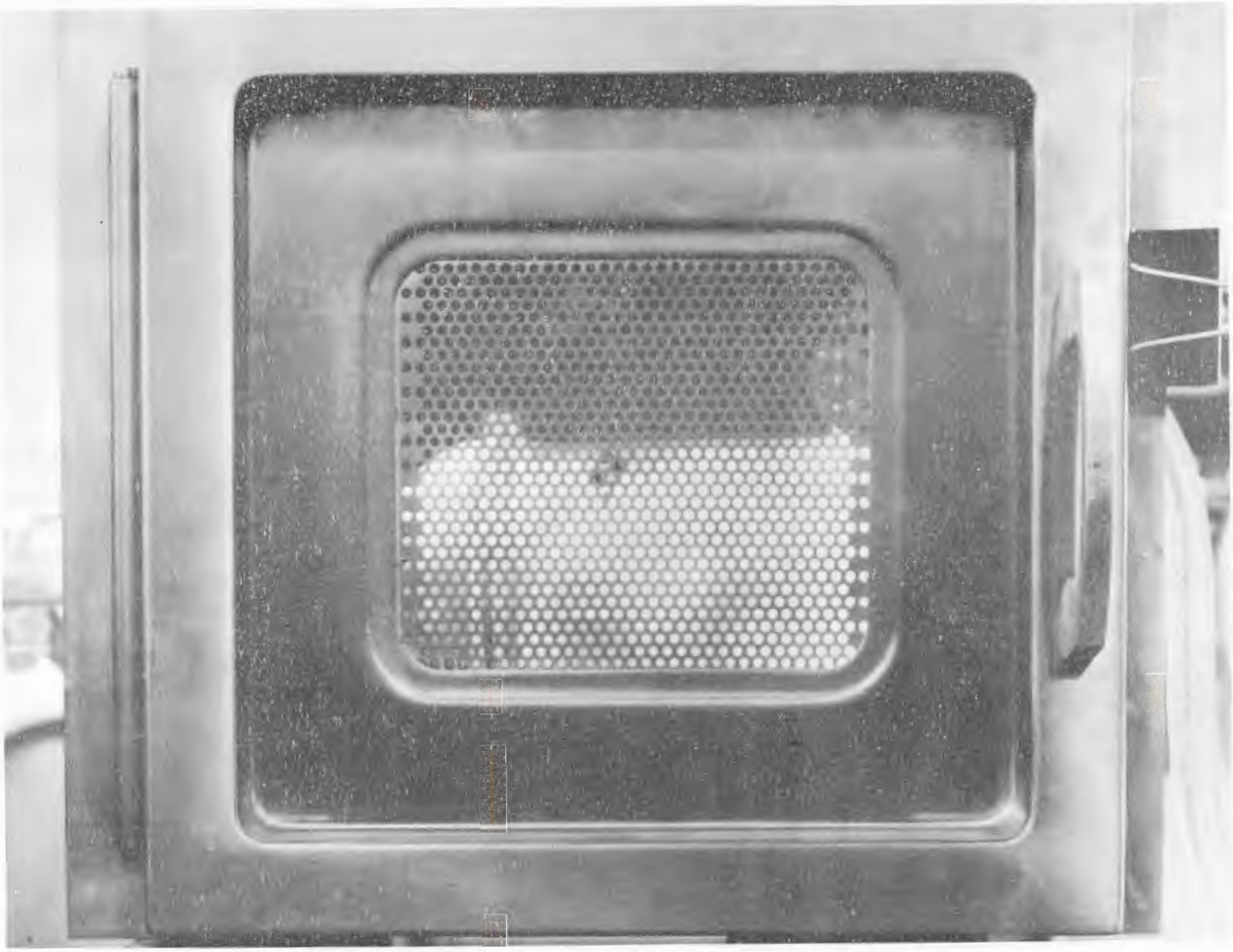

FIG. 1a. Microwave Breakdown in Air.
High power showing maximum corona (at constant pressure).

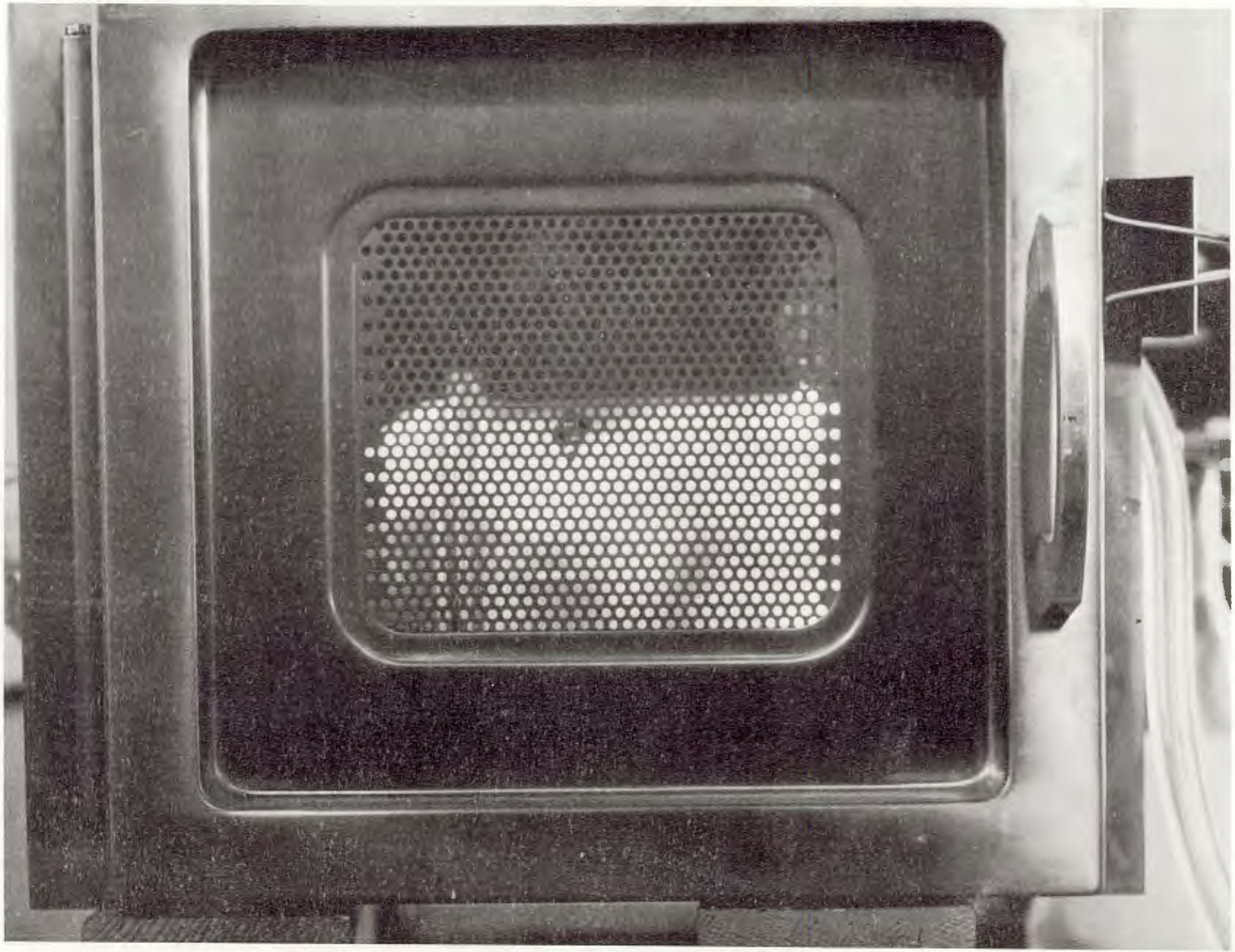

FIG. 1b. Microwave Breakdown in Air.
Medium power showing reduced corona (at constant pressure).

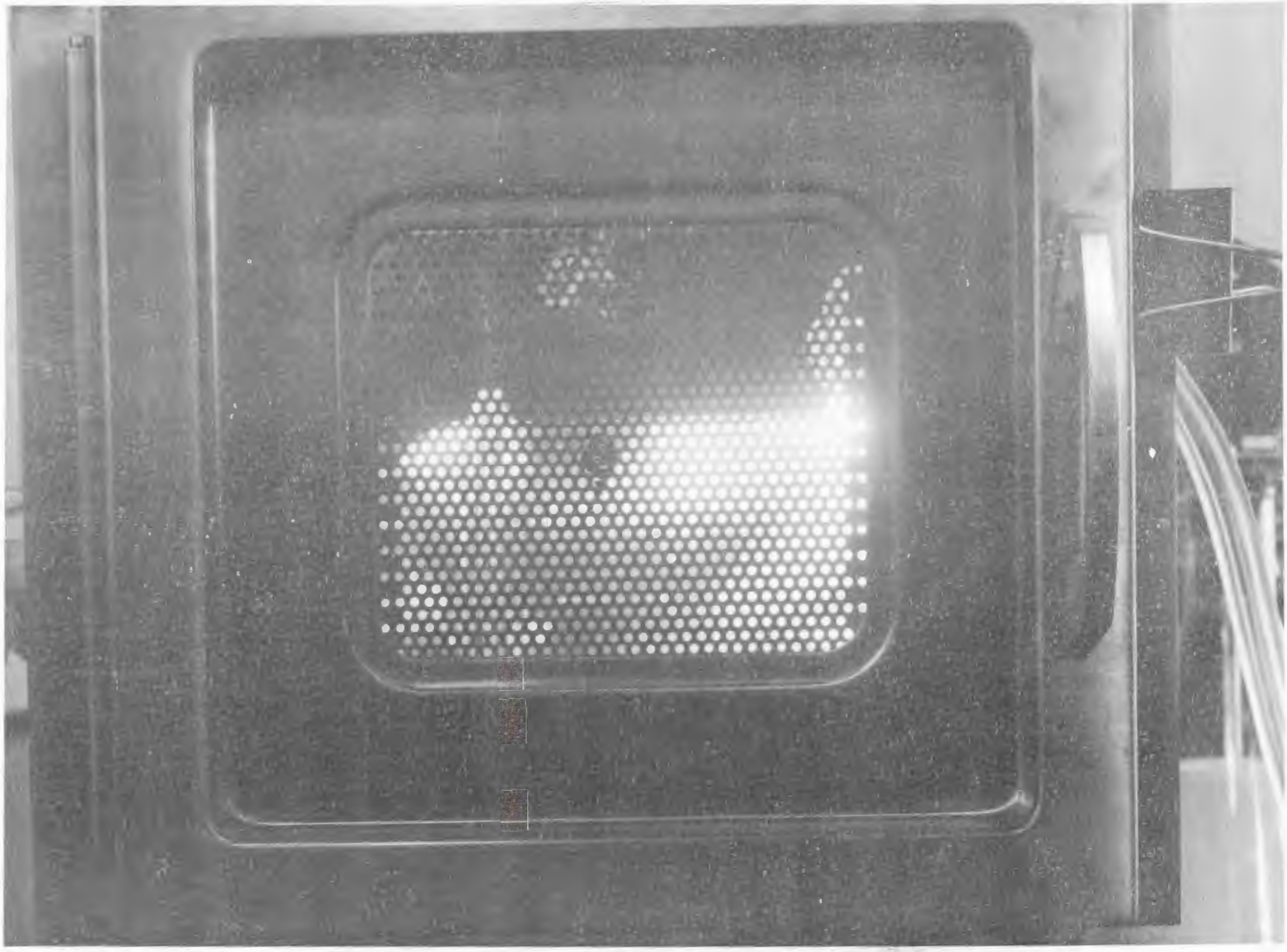

FIG. 1c. Microwave Breakdown in Air.
Low power showing minimum corona. Note isolation of hot spots corresponding to maxima in electric field.

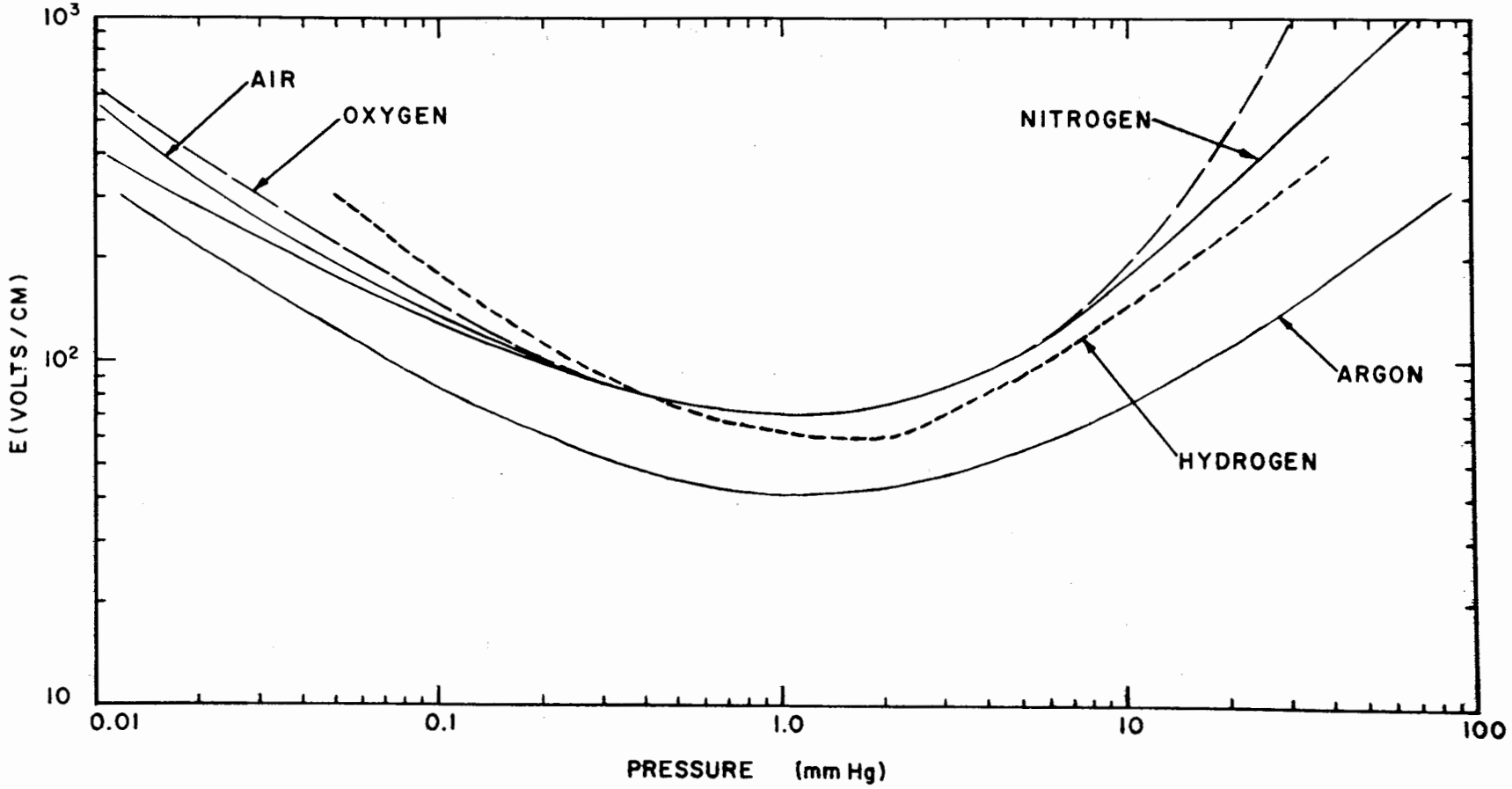

FIG. 2. Microwave in nitrogen, air, oxygen hydrogen, and argon at 994 MHz and = 1.51 cm. A.D. MacDonald, D.U. Gaskell, H.N. Gitterman (1963) PHYREV J1 V130 P.1841

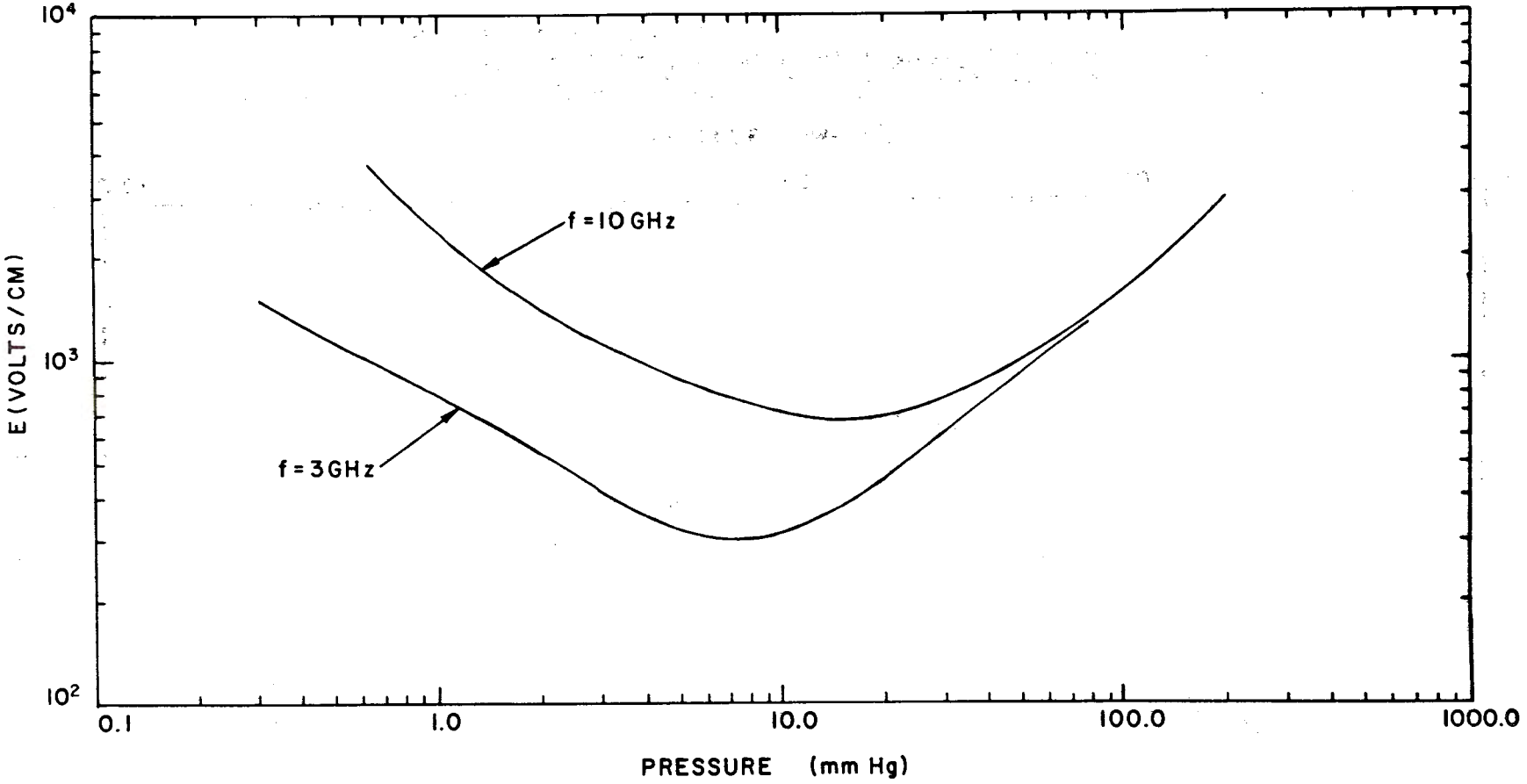

FIG. 3. Breakdown fields as a function of pressure for different frequencies (gas, Heg, a mixture of He and Hg - = 0.6 cm). A.D. MacDonald, Microwave Breakdown in Gases. Wiley & Sons, NY P.7.

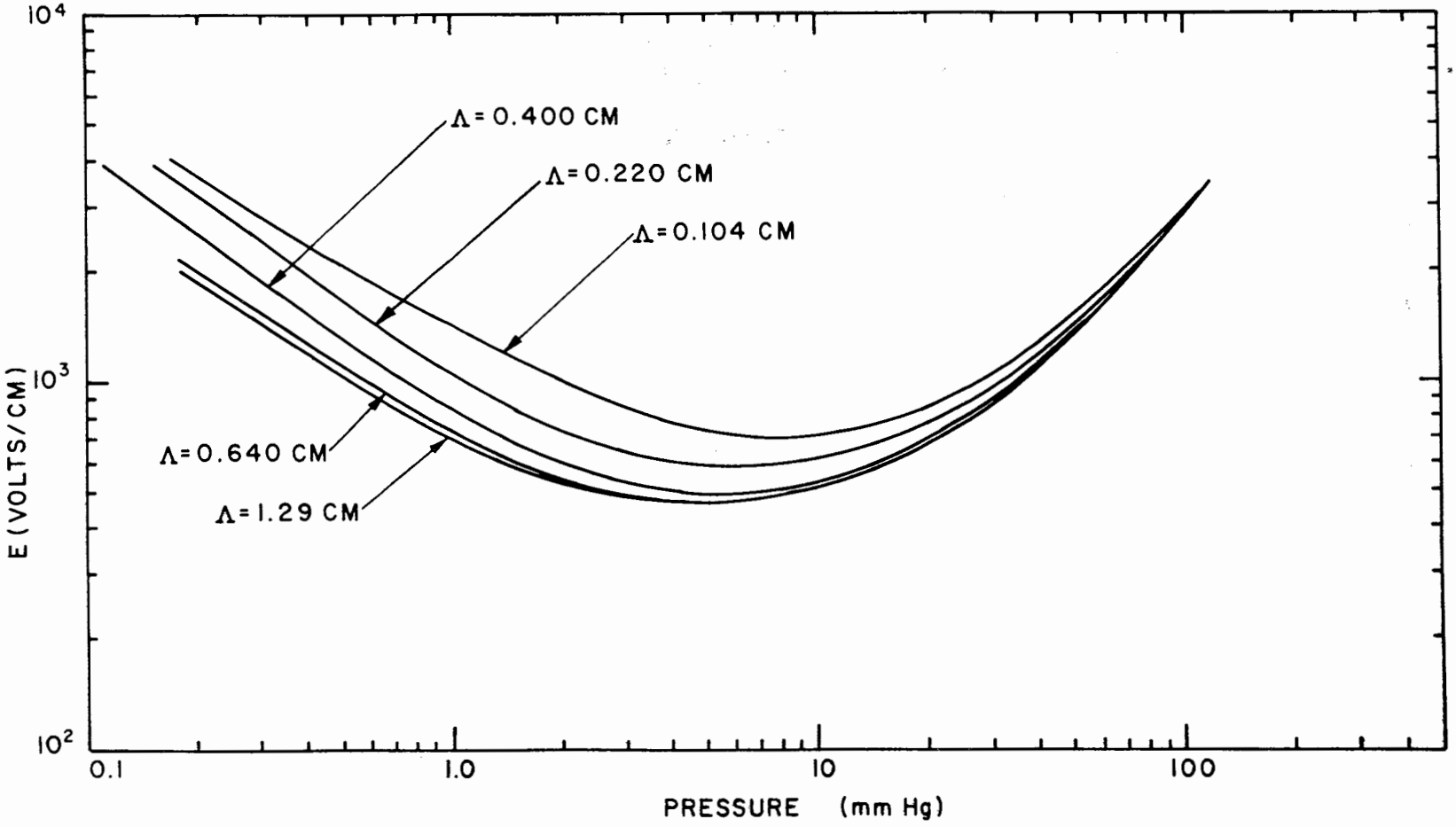

FIG. 4. Microwave Breakdown in Air at 9.4 GHz.
A.D. MacDonald, D.U. Gaskell, H.N. Gitterman (1963)
PHYREV. J1 V13 P.1841

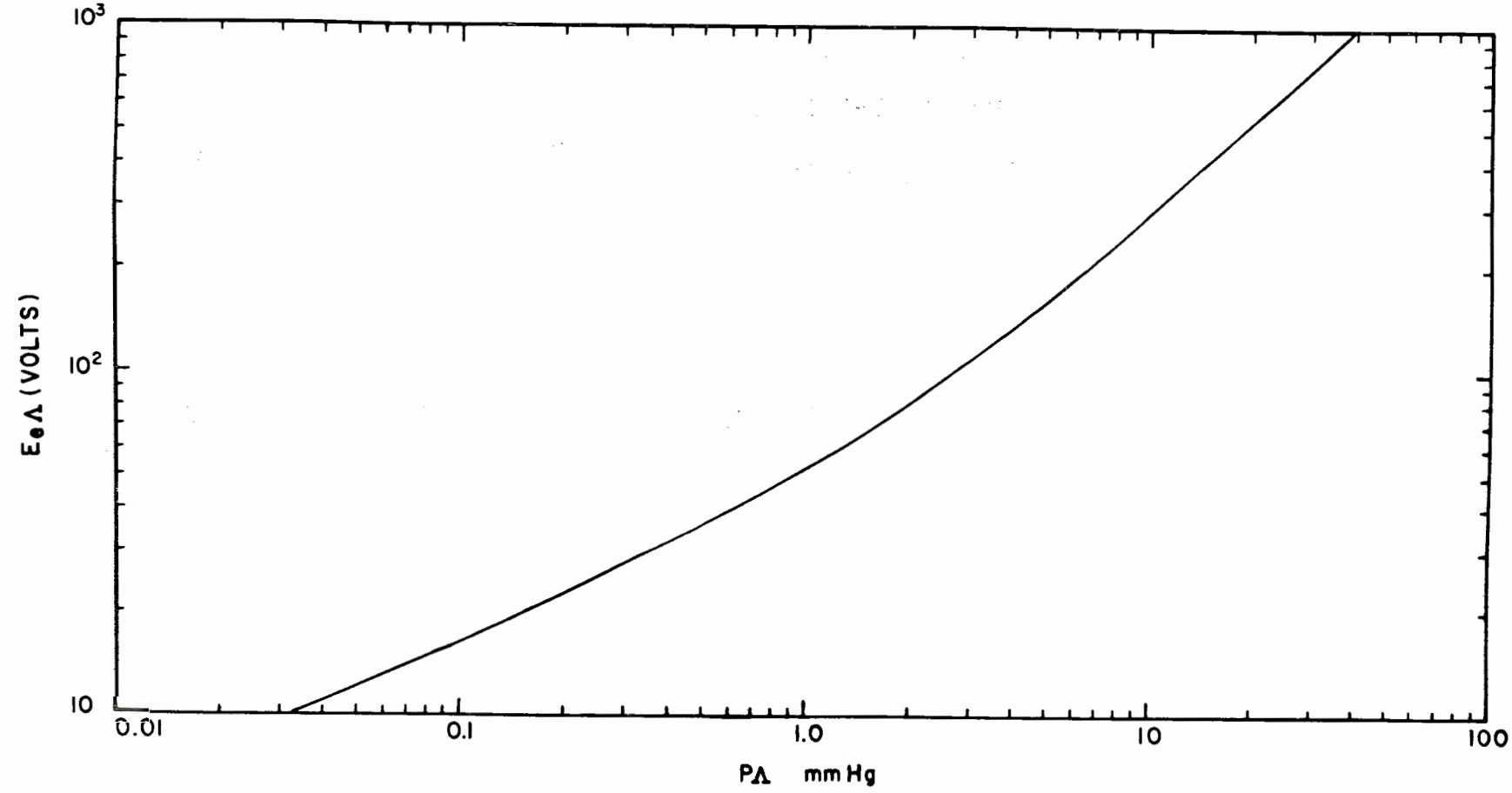

FIG. 5 Microwave Breakdown ($E_{e\ s\ p}$) for Air.
A.D. MacDonald, D.U. Gaskell, H.N. Gitterman (1963)
PHYREV. J1 V130 P. 1841

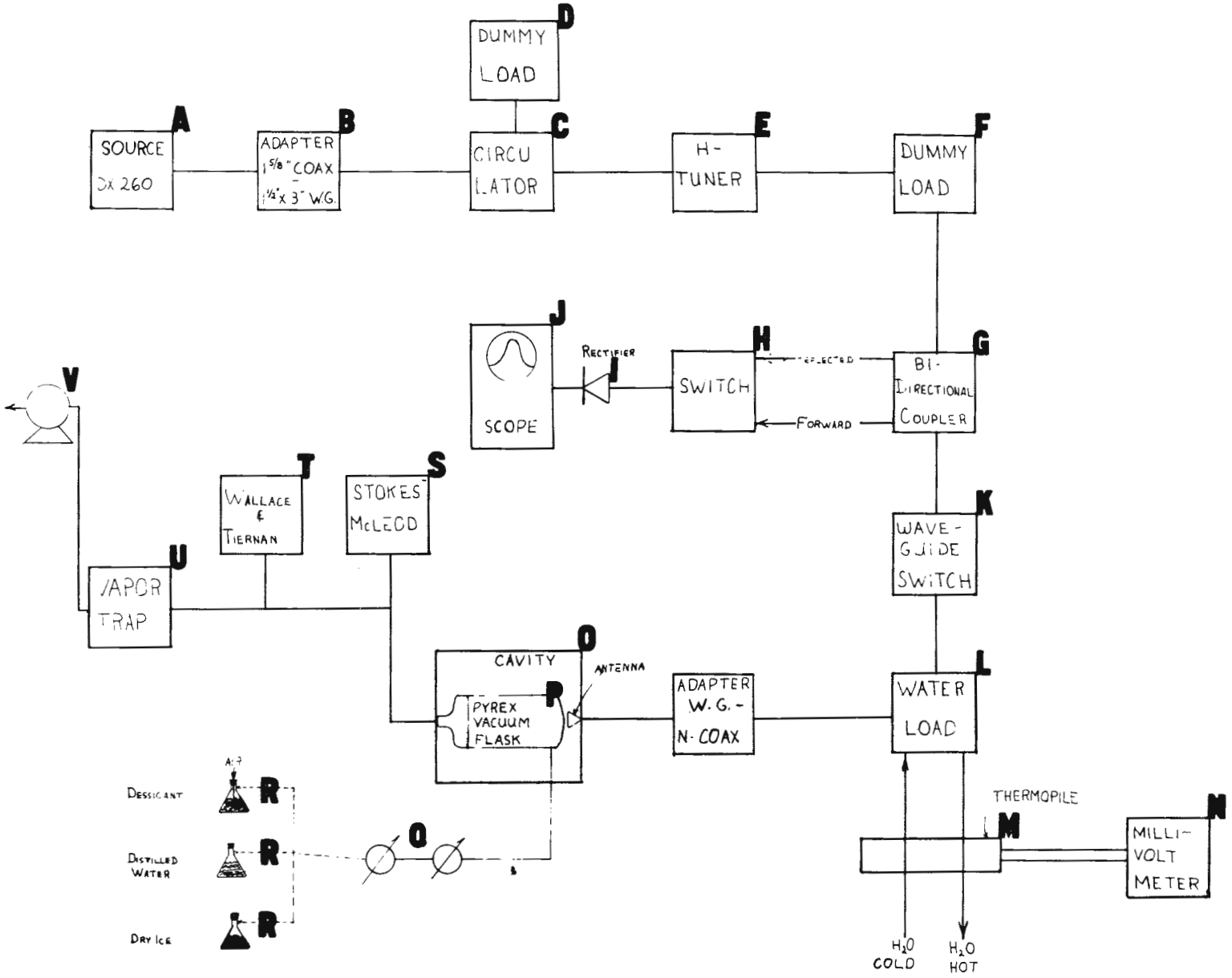

FIG. 6. Experimental set up for determination of microwave breakdown fields - block diagram.

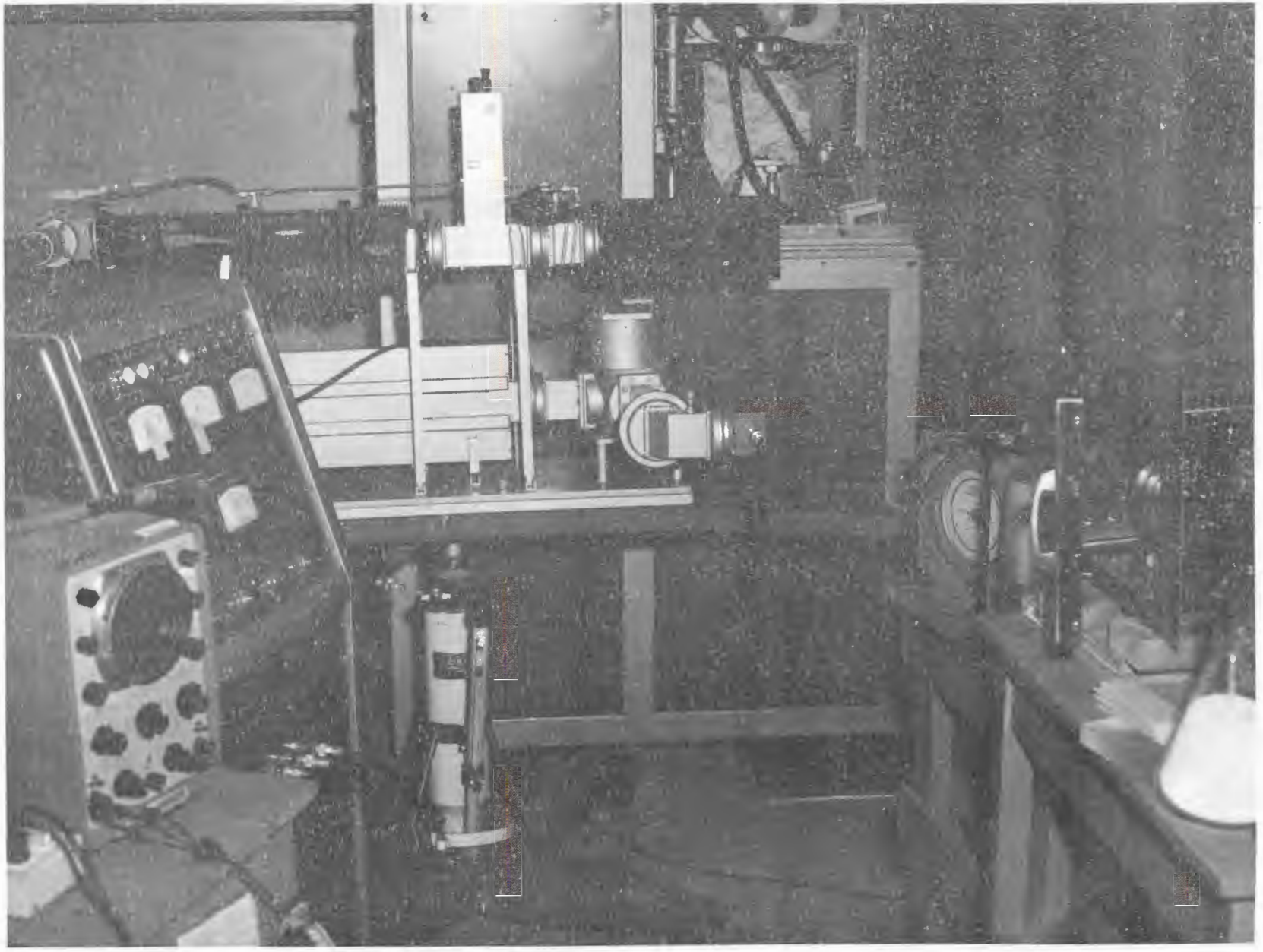

FIG. 7. Photograph of experimental set up for determination of microwave breakdown fields.

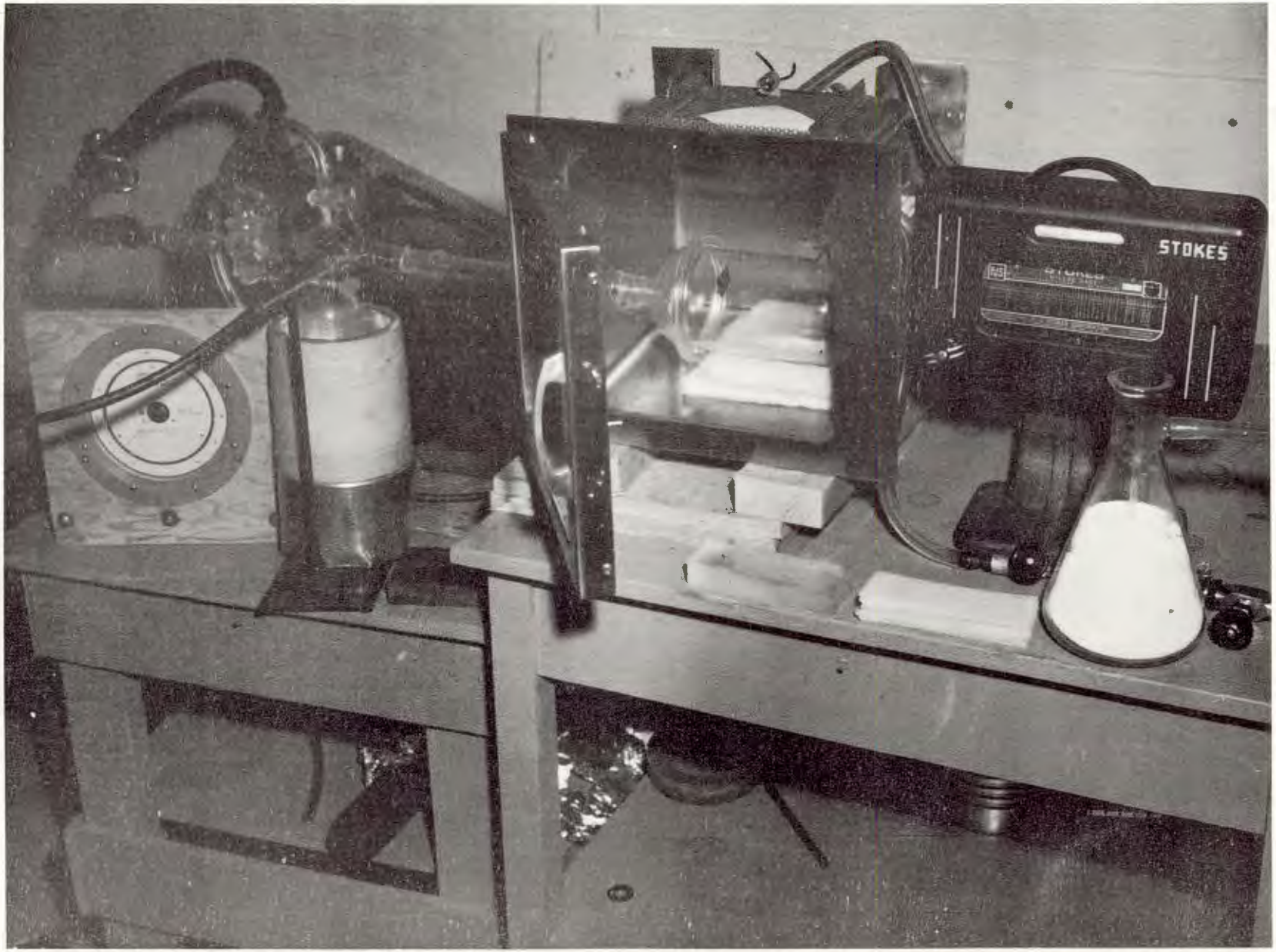

FIG. 8. Microwave cavity and vacuum system for determination of breakdown fields

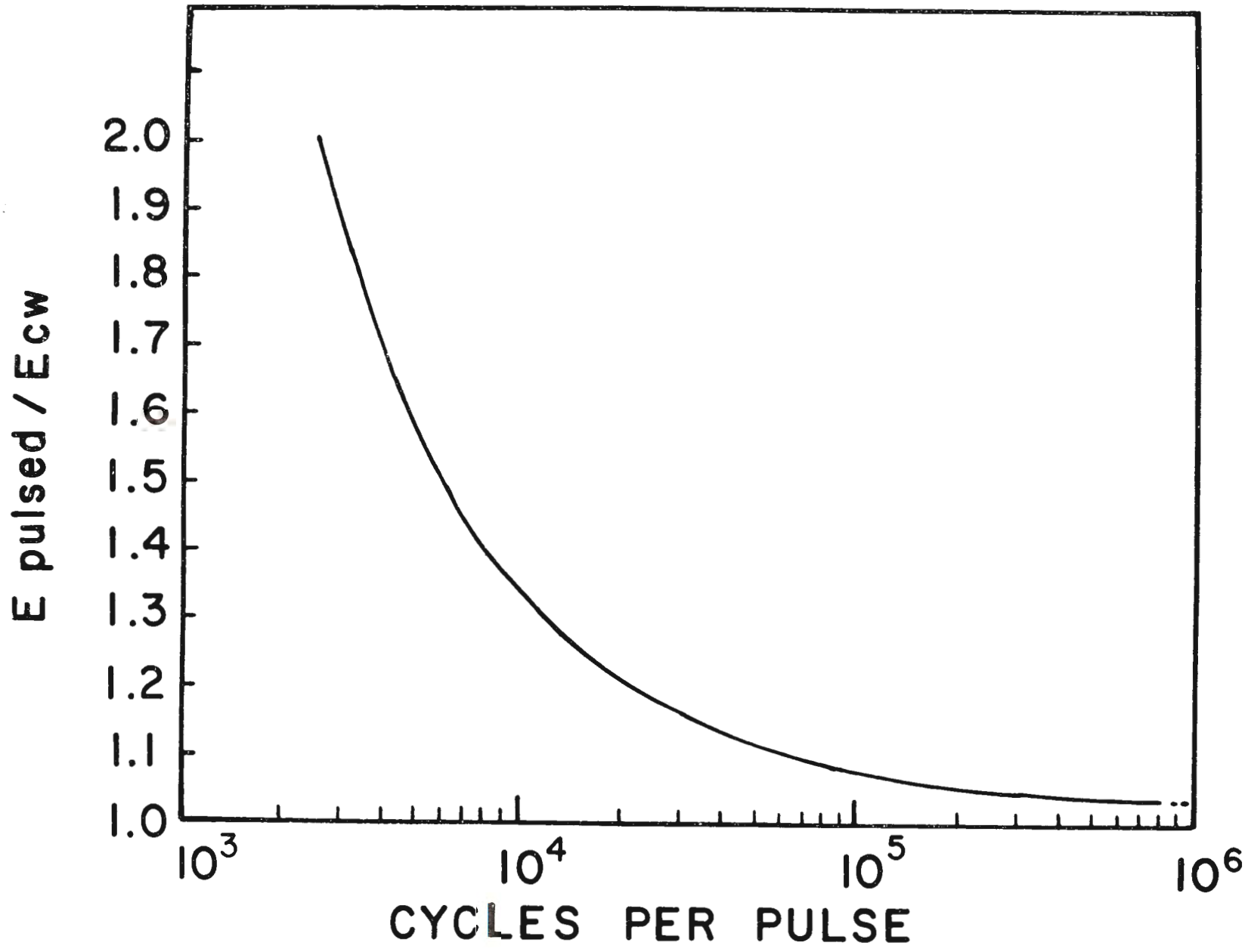

FIG. 9. Ratio of pulsed to CW breakdown for air plotted as a function of cycles per pulse. Frequencies from 0.99 to 24.1 GHz. Data are for pressures near the minima of breakdown curves. A.D. MacDonald, Microwave Breakdown in Gases. Wiley & Sons, NY P 170

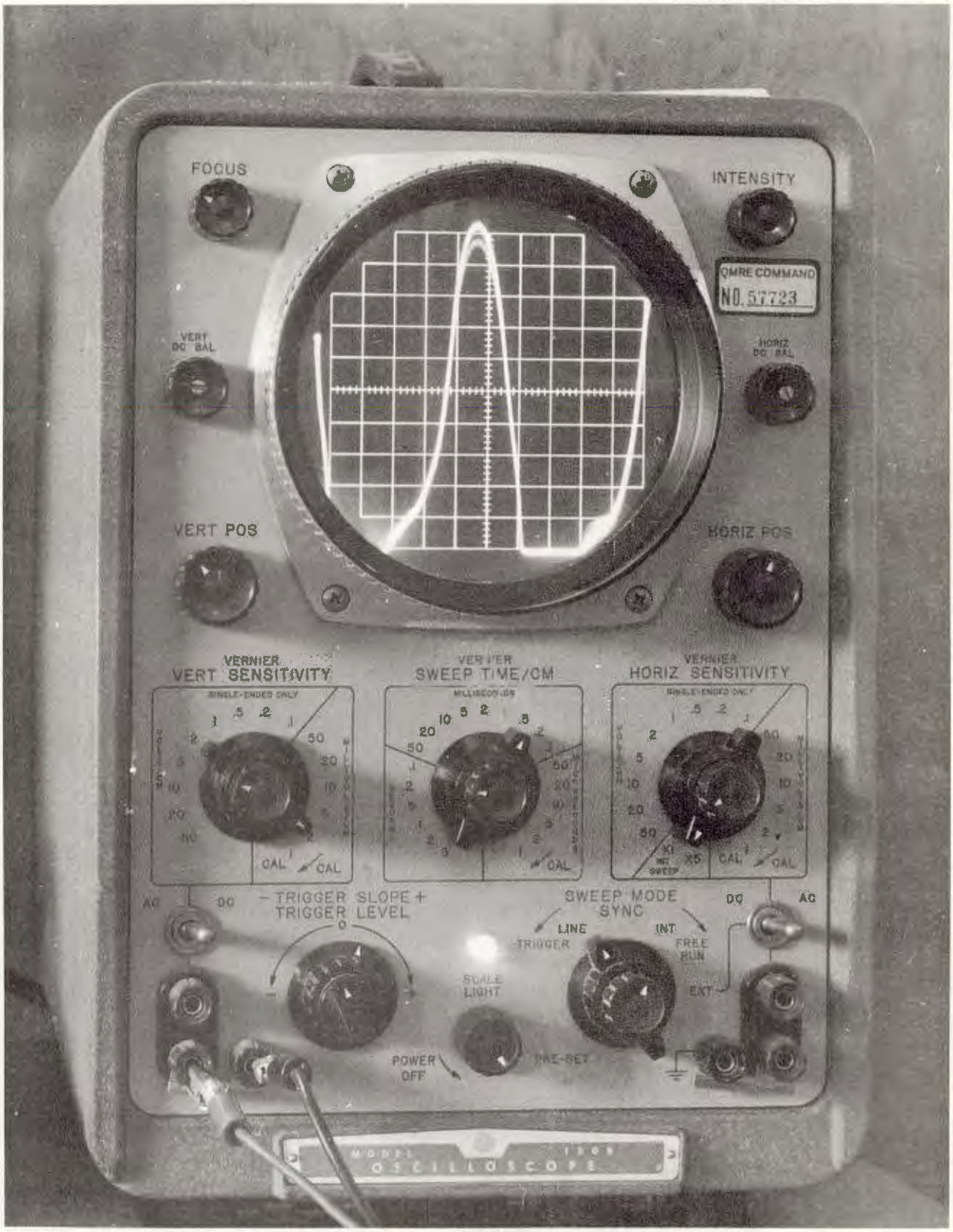

Oscilloscope traces of sampled rf power

FIG. 10a. Forward power.

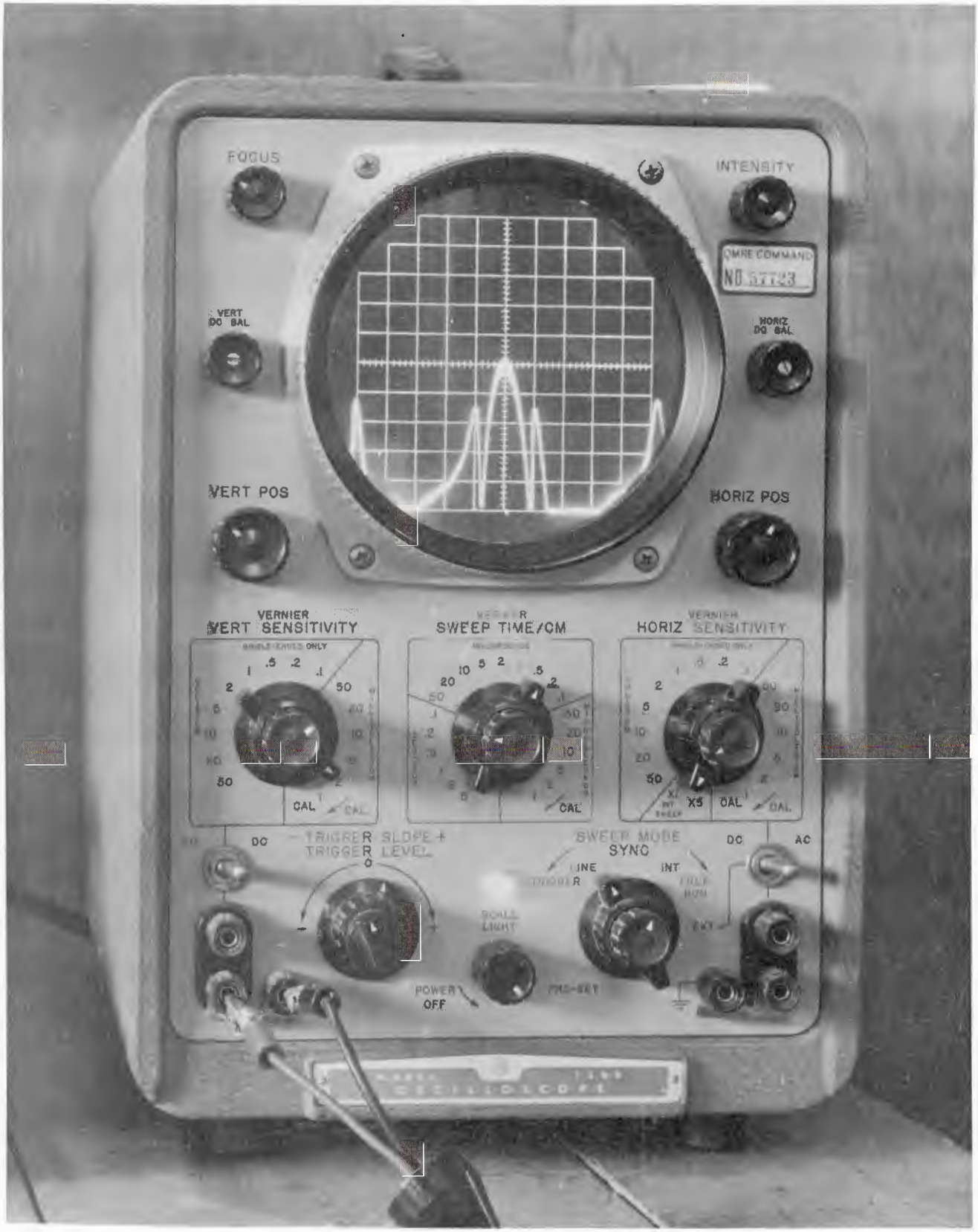

Oscilloscope traces of sampled rf power

FIG. 10b. Reflected power, no breakdown.

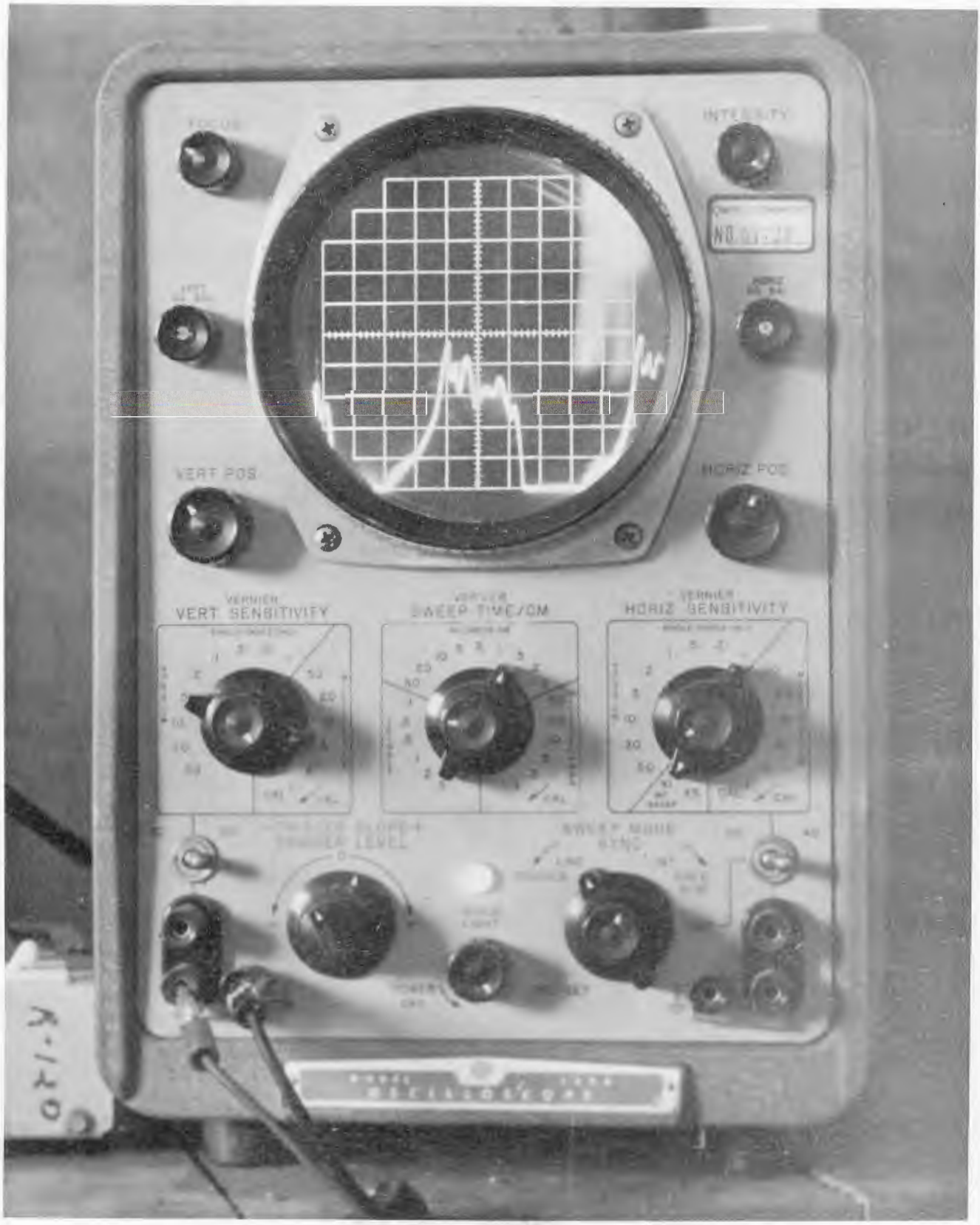

Oscilloscope traces of sampled rf power

FIG. 10c. Reflected power - breakdown.

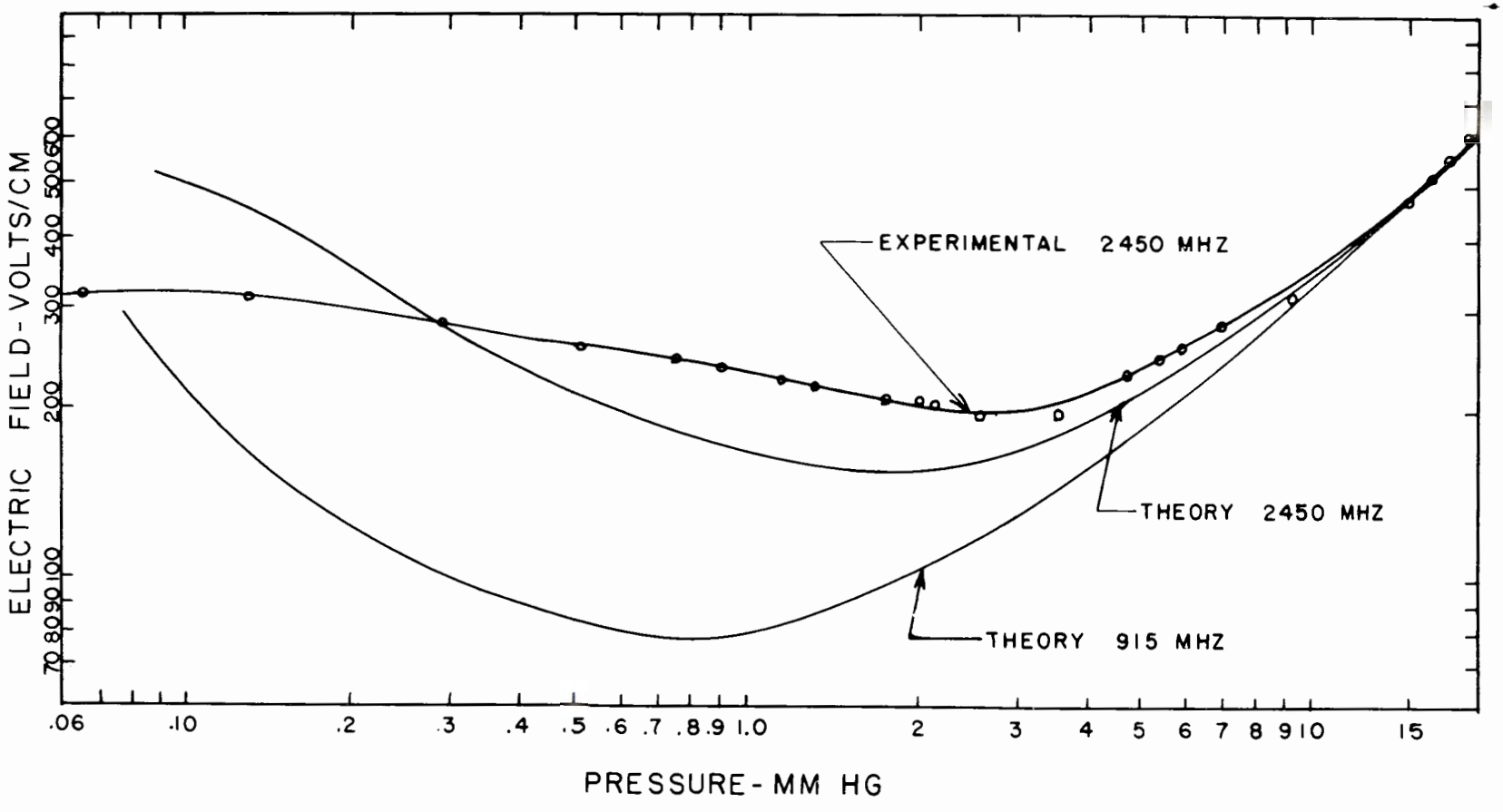

FIG. 11. Experimental and theoretical microwave breakdown in air, = 0.67 cm.

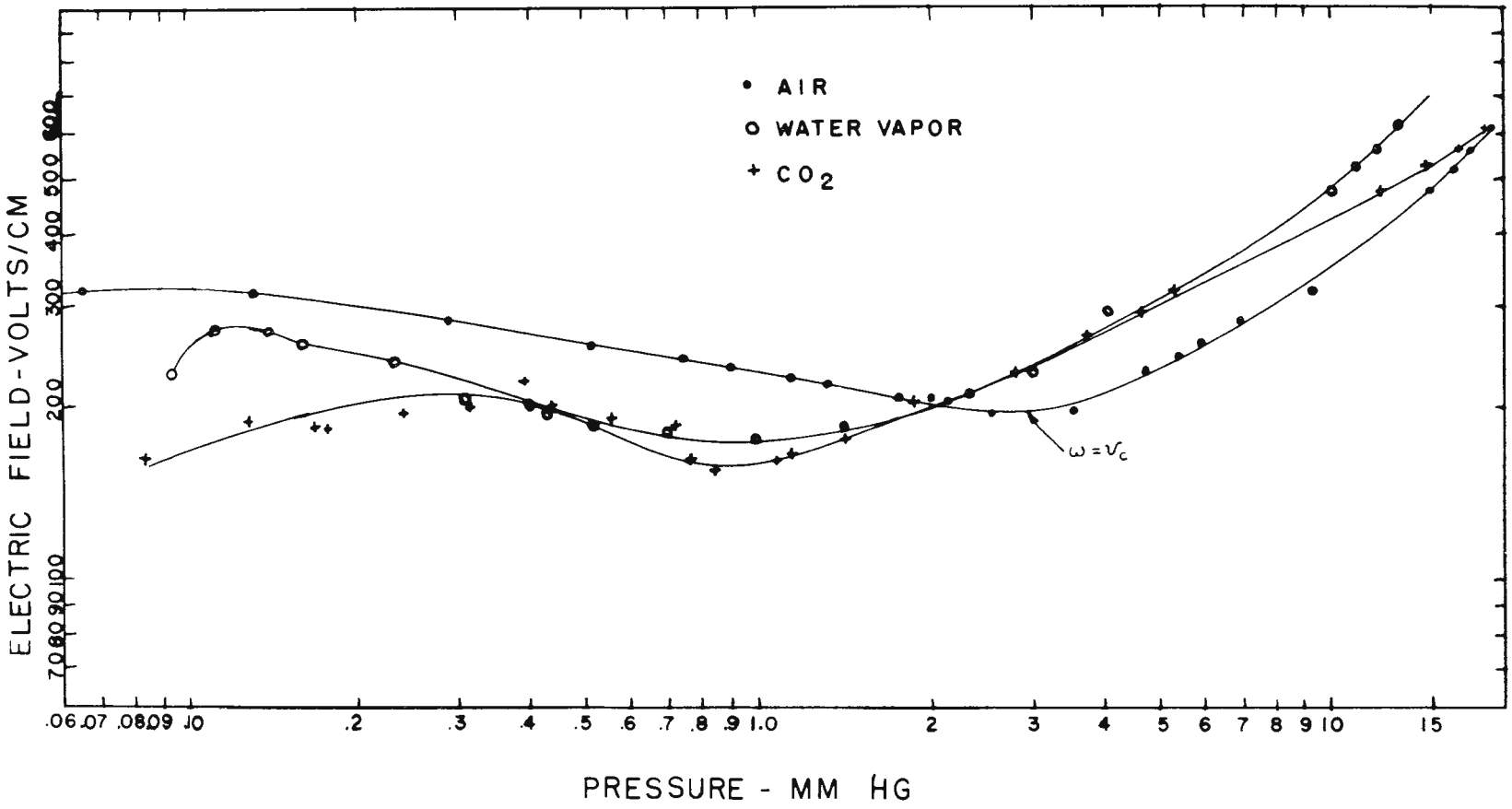

FIG. 12. Experimental microwave breakdown in air, water vapor, and carbon dioxide at 2450 MHz = 0.67 cm.

FOOD LABORATORY INTERNAL DISTRIBUTION LIST

Process Development

Copies		
25	-	Chief, Technical Plans Office, NLABS (20 for transmittal to Defense Documentation Center)
2	-	Technical Library, NLABS
10	-	Program Coordination Office, Food Laboratory, NLABS
7	-	Division Chiefs, Food Laboratory, NLABS
2	-	Marine Liaison Officer, NLABS
3	-	Air Force Liaison Officer, NLABS
1	-	Director, Earth Sciences Laboratory, NLABS
2	-	Director, General Equipment and Packaging Laboratory, NLABS
3	-	Director, Pioneering Research Laboratory, NLABS
	-	Project Officer and Alternate Project Officer, Food Lab, NLABS

FOOD LABORATORY DISTRIBUTION LIST

Process Development

Copies

1 - Commanding General
US Army Medical Research
and Development Command
ATTN: MEDDH-SI
Washington, D.C. 20315

2 - Commanding General
US Army Test and Evaluation Command
ATTN: AMSTE-BC
Aberdeen Proving Ground, MD 21005

1 - Commanding General
US Army Combat Development Command
Combat Service Support Group
Fort Lee, VA 23801

1 - Commanding General
US Army Combat Development Command
ATTN: CDCMR-O
Fort Belvoir, VA 22060

1 - Commanding General
US Army Materiel Command
ATTN: AMCRD-J1
Department of the Army
Washington, DC 20315

2 - Commanding Officer
Edgewood Arsenal
ATTN: SMUEA-TSTI-TL
Edgewood Arsenal, MD 21010

Copies

1 - Commanding Officer
US Army Medical Nutrition Laboratory
Fitszimons General Hospital
Denver, CO 80240

1 - Commander
Defense Personnel Support Center
ATTN: Directorate of Subsistence,
DPSC-STS
2800 South Street
Philadelphia, PA 19101

1 - Commandant of the Marine Corps
Code A04D
Washington, D.C. 20380

1 -Commandant of the Marine Corps
ATTN: Code CDE
Washington, DC 20380

1 - Executive Secretary
Interdepartmental Committee on
Radiation Preservation of Food
Consumer Products Division 623
Business and Defense Service Admin.
US Department of Commerce
Washington, DC 20230

2 - Director
Development Center
Marine Corps Development and
Education Command
ATTN: Combat Service Support Division
Quantico, VA 22134

Copies

1 - Director
Division of Biology and Medicine
US Atomic Energy Commission
Washington, D.C. 20545

1 - Director
US Army Advanced Material
Concepts Agency
Washington, D.C. 20315

1 - Chief, Life Sciences Division
Army Research Office
Office of Chief of Research
and Development
Washington, D.C. 20310

3 - Office of the Coordinator of Research
University of Rhode Island
Kingston, Rhode Island 02881

1 - Dr. Herbert E. Hall
Chief, Food Microbiology
National Center for Urban and
Industrial Health
Food Protection Research
222 East Central Parkway
Cincinnati, Ohio 45202

1 - Stimson Library
ATTN: Documents Librarian
US Army Medical Field Service School
Brooke Army Medical Center
Fort Sam Houston, TX 78234

Copies

1 - Library Southern Utilization
Research and Development Division
Agricultural Research Service
US Department of Agriculture
P O Box 19687
New Orleans, LA 70119

2 - Quartermaster School Library
US Army Quartermaster School
Fort Lee, VA 23801

2 - Technical Library
USACDC Institute of Land Combat
301 Taylor Drive
Alexandria, VA 22314

1 - US Department of Agriculture
Division of Acquisitions
National Agriculture Library
Washington, D.C. 20250

2 - US Army Research Office
ATTN: Technical Library
3045 Columbia Pike
Arlington, VA 22040

2 - Headquarters 12th Support Brigade
ACofS Services
ATTN: Food Advisor
Fort Bragg, NC 28307

4 - Exchange and Gift Division
Library of Congress
Washington, D.C. 20540

UNCLASSIFIED
Security Classification

DOCUMENT CONTROL DATA - R & D

(Security classification of title, body of abstract and indexing annotation must be entered when the overall report is classified)

1. ORIGINATING ACTIVITY *(Corporate author)*
U.S. Army Natick Laboratories
Natick, Massachusetts 01760

2a. REPORT SECURITY CLASSIFICATION
UNCLASSIFIED

2b. GROUP

3. REPORT TITLE
MICROWAVE APPLICATIONS TO FREEZE DEHYDRATION-GASEOUS BREAKDOWN VS ELECTRIC FIELD STRENGTH

4. DESCRIPTIVE NOTES *(Type of report and inclusive dates)*

5. AUTHOR(S) *(First name, middle initial, last name)*
James W. Gould
Ernest M. Kenyon

6. REPORT DATE	7a. TOTAL NO. OF PAGES	7b. NO. OF REFS
October 1970	57	34

8a. CONTRACT OR GRANT NO.

b. PROJECT NO.
1J662708D553

c.

d.

9a. ORIGINATOR'S REPORT NUMBER(S)

9b. OTHER REPORT NO(S) *(Any other numbers that may be assigned this report)*
71 - FL FL - 117

10. DISTRIBUTION STATEMENT
This document has been approved for public release and sale; its distribution is unlimited.

11. SUPPLEMENTARY NOTES

12. SPONSORING MILITARY ACTIVITY
U.S. Army Natick Laboratories
Natick, Massachusetts 01760

13. ABSTRACT

The use of microwave energy can reduce freeze-drying cycles to 1/2 - 1/10 of the time required for conventional freeze-drying. Two drawbacks to design and application of microwave energy to freeze-drying are determination of the electric field available for dielectric heating and corona breakdown (gas plasma formation). Corona breakdown can cause undesirable effects in food products during freeze-dehydration, such as deterioration of flavor components and degrading of structure. The author reviews the theory of microwave gas breakdown and compares theoretical and literature breakdown curves for air and noble gases to show the effects of pressure, temperature, frequency, gas composition size and shape of cavity, and electric field strength, and derives an equation which shows the effect of a dielectric load in the cavity on gas breakdown, showing how this relates to heating of the dielectric load and to electric field strength. Experimental breakdown curves for air, water and carbon dioxide are given and related to theory at 2450 MHZ. Pressures studied were in the range of 10 to 20 Torr, which covers the region of practical freeze-drying. A single cavity approximately two wavelengths on each side was used for 3 gases. Electric field strengths were varied from 150 to 600 volts/cm. A vacuum flask inside the cavity contained the corona. The agreement between theory and experiment is good, both for air breakdown and the effect of a dielectric load. The results obtained show just how much power can be applied and absorbed by the food without corona breakdown. This plus a knowledge of maximum mass transfer rates of water vapor across the dried food layer is expected to enable theoretical optimization and prediction of microwave freeze-drying rates.

DD FORM 1 NOV 68 1473 REPLACES DD FORM 1473, 1 JAN 64, WHICH IS OBSOLETE FOR ARMY USE.

UNCLASSIFIED
Security Classification

14. KEY WORDS	LINK A		LINK B		LINK C	
	ROLE	WT	ROLE	WT	ROLE	WT
Pressure	6					
Temperature	6					
Gas	6,7		9			
Dimensions	6					
Shape	6					
Cavities	6					
Electrical properties	6					
Dielectrical properties	6					
Microwaves	6, 10		5			
Freeze-drying	8,7		4			
Coronas			9			
Breakdown			8			
Curves			8			